1.0

1.1

1.25

2.8

3.2

3.6

2.5

2.2

2.0

1.4

1.8

1.6

MICROCOPY RESOLUTION TEST CHART

LEVEL

R–1434

MATERIALS RESEARCH FOR ADVANCED
INERTIAL INSTRUMENTATION

TASK 2: GAS BEARING MATERIAL DEVELOPMENT

DECEMBER 1980

TECHNICAL REPORT NO. 3
FOR THE PERIOD
1 OCTOBER 1979 – 30 SEPTEMBER 1980

BY

D. DAS, K. KUMAR, E. WETTSTEIN, J. WOLLAM

DTIC
APR 27 1981

The Charles Stark Draper Laboratory, Inc.
Cambridge, Massachusetts 02139

81 4 27 099

REPORT DOCUMENTATION PAGE		READ INSTRUCTIONS BEFORE COMPLETING FORM
1. REPORT NUMBER Technical Report No. 3	**2. GOVT ACCESSION NO.** AD-AC98229	**3. RECIPIENT'S CATALOG NUMBER**
4. TITLE *(and Subtitle)* MATERIALS RESEARCH FOR ADVANCED INERTIAL INSTRUMENTATION. TASK 2, GAS BEARING MATERIAL DEVELOPMENT.		**5. TYPE OF REPORT & PERIOD COVERED** Technical Report 1 Oct 1979 — 30 Sept 1980
		6. PERFORMING ORG. REPORT NUMBER
7. AUTHOR(s) D. Das, K. Kumar, E. Wettstein, J. Wollam		**8. CONTRACT OR GRANT NUMBER(s)** N00014-77-C-0388
9. PERFORMING ORGANIZATION NAME AND ADDRESS The Charles Stark Draper Laboratory, Inc. Cambridge, Massachusetts 02139		**10. PROGRAM ELEMENT, PROJECT, TASK AREA & WORK UNIT NUMBERS**
11. CONTROLLING OFFICE NAME AND ADDRESS Office of Naval Research Department of the Navy 800 N. Quincy St., Arlington, Virginia 22217		**12. REPORT DATE** December 1980
		13. NUMBER OF PAGES 104
14. MONITORING AGENCY NAME & ADDRESS *(if different from Controlling Office)* Office of Naval Research 666 Summer St. Boston, Massachusetts 02210		**15. SECURITY CLASS.** *(of this report)* UNCLASSIFIED
		15a. DECLASSIFICATION/DOWNGRADING SCHEDULE

16. DISTRIBUTION STATEMENT *(of this Report)*

Approved for public release, distribution unlimited.

17. DISTRIBUTION STATEMENT *(of the abstract entered in Block 20, if different from Report)*

DTIC
SELECT
APR 27 1981

18. SUPPLEMENTARY NOTES

19. KEY WORDS *(Continue on reverse side if necessary and identify by block number)*

Beryllium	Boron	Beryllium-Ceramic Composite
Ion Implantation	Reactive Diffusion	Hot Isostatic Pressing (HIP)
CVD	Metal Matrix Composite	

20. ABSTRACT *(Continue on reverse side if necessary and identify by block number)*

Progress is reported on three fronts: Boron deposition on beryllium by chemical vapor deposition (CVD) and subsequent reactive diffusion of the deposited boron film, ion implantation of boron into beryllium, and beryllium-ceramic composite materials.

CVD coatings of boron, from B_2H_6 on beryllium at 700°C showed less tendency to crack and spall at a 5 µm thickness than did previous coatings 1 µm thick which had been deposited at 900°C and 950°C. Hardness also increased for the lower temperature thicker films; 2500 KHN versus 1400 KHN.

DD FORM 1473 EDITION OF 1 NOV 65 IS OBSOLETE
1 JAN 73

Improved beryllium surface coverage resulted from redesigning the CVD processing chamber to minimize oxygen contamination by providing for vacuum bake out. Films of 10 μm, 3000 KHN, are now obtained without cracking or spalling.

Metallography electron diffraction and Auger analysis suggest that the coatings consist of an amorphous outer layer of boron with a layer of mixed beryllium borides at the interface. Heat treatment at 900°C for several hours brought about conversion to BeB_6. Future studies will use more rigorous conditions in an attempt to form BeB_2, with the objective of allowing selection of B, BeB_2, or BeB_6 as a gas bearing surface. Emphasis will also be placed on generation of new information pertaining to diffusion kinetics in the Be-B system.

Boron-implanted I-400 beryllium sample preparation and evaluation proceeded, on both uniform concentration and graded concentration layers. The latter type, innovated in this program, are prepared either with multiple implants or by implanting boron ions through a sputter-deposited boron film, and are seen as promising the most effective wear surfaces for the least processing time. Difficulties in attaining the desired degree of flatness and finish on the starting material were encountered and overcome.

Implanted sample surface profile and appearance, as well as apparent hardness, were found to be strongly dependent on the effectiveness of substrate heat dissipation and on the quality of the vacuum environment prevailing during implantation.

Friction and wear measurements against a hardened steel pin showed that all of the implanted discs tested were greatly improved in their wear resistance over both untreated beryllium and plasma-sprayed Al_2O_3, even where the implant was very shallow, with the best overall performance found for a 40 a/o dose. No proof of beryllium boride compound formation has yet been obtained but a new technique entailing both Auger sputter-profiling and reflection electron diffraction will be applied to the search.

Development of a metal-matrix, beryllium-ceramic composite for use as a gas bearing material was introduced into the program in October 1979. The ceramics chosen for examination were Al_2O_3, TiC, and TiB_2. Use of powder metallurgy/hot isostatic pressing (HIP) technique resulted in a ceramic particle dispersion in a beryllium matrix. High energy blending procedures for mixing the powders coupled with high temperature outgassing of the powders prior to container encapsulation yielded densified billets with reasonably uniform microstructures, and some samples approached theoretical density. It was determined that -325 mesh ceramic (TiB_2) powder was more preferred than was the 1 to 2 μm size powder (for HIPing with -325 mesh beryllium powder) because a more uniform dispersion with individual ceramic particles properly bonded to the beryllium matrix resulted in the former from processing. The microstructure of the latter (containing 1 to 2 μm ceramic particles) in contrast, consisted of the ceramic particles mainly clustered at the grain boundaries of the beryllium with less than desired bonding to the matrix. This study also showed that wetting of the Al_2O_3 particles by the beryllium was poor and this resulted in ceramic particle pull-out during polishing. Micromachining of ceramic particles during lapping was observed in the -325 mesh TiB_2 particle composite. (These particles were well bonded to the matrix.) High density billets of TiC containing composites could not be produced by this process and this was explained on inadequate outgassing of these powders. Future work in this study will be mainly concentrated on the TiB_2 containing composite materials.

R-1434

MATERIALS RESEARCH FOR ADVANCED INERTIAL INSTRUMENTATION

TASK 2: GAS BEARING MATERIAL DEVELOPMENT

DECEMBER 1980

TECHNICAL REPORT NO. 3

FOR THE PERIOD

1 October 1979 - 30 September 1980

D. Das, K. Kumar, E. Wettstein, J. Wollam

Approved:

M.S. Sapuppo, Head
Component Development Department

The Charles Stark Draper Laboratory, Inc.
Cambridge, Massachusetts 02139

ACKNOWLEDGEMENT

Accession For
NTIS GRA&I
DTIC TAB
Unannounced
Justification

By
Distribution/
Availability Codes
Avail and/or
Special

Dist

A

TABLE OF CONTENTS

LIST OF ILLUSTRATIONS

LIST OF ILLUSTRATIONS (Continued)

LIST OF TABLES

SECTION 1.

INTRODUCTION

In the construction of gyroscopic inertial instruments, the purely structural requirements with respect to strength, stiffness, and creep can be met for most purposes through the use of instrument-grade beryllium, but the mating surfaces of gas-bearings demand higher hardness and greater wear resistance than beryllium offers. This discrepancy has been met in past and present instrument designs in a variety of ways, but operational and processing problems continue to persist and a better materials system is needed. The present task addresses this latter requirement through research efforts on new materials and processes for gyroscopes with gas bearings.

In general, the materials which are hard enough for use in gas bearings are also physically incompatible with the other structural members of the instrument assembly. Differences in thermal expansion characteristics and low values of thermal conductivity of these materials result in undesirable strains and temperature variations in the assembly. This leads to a variety of instrument instabilities which adversely affect the accuracy and reliability of the several inertial components.

Gas bearings initially built at The Charles Stark Draper Laboratory, Inc. (CSDL) involved fabricating entire bearings out of solid pieces of ceramic. These ceramics were typically produced by sintering and hot pressing techniques. Difficulties were encountered in machining these materials, making the process expensive and time consuming. The high cost in money and time, in addition to the problems stemming from low values of thermal expansion and thermal conductivity for ceramics, caused this option to be discarded.

The subsequent rationale developed to resolve the discrepancies envisioned the use of two different materials, since no single material was known to meet all demands. One material was to form the structural member and satisfy bulk property requirements and the other was to be deposited as a coating to yield a low-friction, wear-resistant surface for the gas bearing.

SECTION 2.

MATERIALS PROPERTY REQUIREMENTS

2.1   Bulk Properties

        Since the basic structure of the instruments consists largely
of beryllium, this material is also the best choice for the structures
supporting the gas bearing surfaces. The bulk property requirements
which it meets are:

        (1) High strength-to-density ratio (important from design
             considerations).

        (2) High thermal conductivity (to avoid temperature
             gradients).

        (3) Nonmagnetic (to eliminate interference with
             electromagnetic circuitry).

        (4) Thermal expansion compatibility with other structural
             members.

        (5) Finishable to accurate tolerances of better than
             1 microinch.

2.2   Coating Properties

        With respect to the material to be applied to the gas bearing
surface as a coating, ideally it would be very similar in its own bulk
properties to those of the underlying structure. For that reason, the
above listing also applies to the coating material, although less

3

critically so where thinner coatings are considered. On the other hand, considerably greater importance must be attached to the surface properties, the most significant of which are:

(1) High resistance to wear from sliding, erosion, and impact, for extended bearing life and stable performance.

(2) Low coefficient of friction for minimum starting torque.

(3) Zero surface porosity, for maximum gas bearing stiffness and minimum contamination entrapment.

2.3   Coating Technology

Materials which are hard enough to be of interest as wear-resistant coatings will generally have such high melting temperatures as to require special methods of application. Two methods which have received attention in this area are plasma-spraying and sputtering, the former enjoying the wider use in production. With plasma spraying it is easy to apply coatings which are several thousandths of an inch thick, while the thicknesses of sputtered films are generally less than that by about two orders of magnitude. On this basis, the two methods are frequently classified as "thick film" and "thin film." Examples of the use of these processes are the plasma-sprayed chromium oxide and aluminum oxide coatings now in use in several instrument designs and the sputter-deposited tungsten carbide and titanium carbide coatings that have been subjects of some past development activity.

2.4   Limitations of Present Technology

The one feature common to both sprayed and sputtered coatings is the difference in physical properties between the coating and the substrate. While this may be somewhat tolerable in thin films produced by sputtering, thicker films made by spraying are susceptible to failure

4

from imperfect match of expansion coefficients at the coating-substrate interface. To reduce stresses that result from differences in expansion coefficients, spraying is generally conducted at lower spray temperatures. However, this adversely affects interparticle cohesive strength, which results in pull-outs during polishing and lapping operations, and generation of wear debris in active service. The clearance between the mating parts of a gas bearing is only about 50 microinches so that even the mildest form of wear (mildest by conventional standards) can prove to be catastrophic in gas bearing applications.

A more severe problem that has been found in sprayed deposits is the presence of interconnecting porous structures in the coating. The effect of this interconnected porosity is to provide a shunt path for gas flow such that the hydrodynamic pressure rise is attenuated from that attainable with a nonporous coating[1]*. This, in turn, causes a lower load capacity and stiffness for the gas bearing. In addition to this most severe effect, the porosity at the surface also results in effectively increasing the bearing gap beyond the physical (design) clearance. Although machining problems in sprayed deposits are less than those for sintered products (because parts are sprayed close to final size), they are present albeit to a lesser degree on a small scale.

The adhesion of the coating to the substrate is an important consideration in wear performance. The forces that give rise to adhesion in films made from both these processes can be both mechanical and chemical in nature. The adhesion observed for deposits fabricated using the arc-plasma technology is generally found to be influenced by mechanical interlocking of the film on the external features of a

---

*Superscript numerals refer to references in the List of References.

5

substrate. However, in both cases, chemical forces frequently give rise to stronger interfacial bonds. This type of bond is often termed a metallurgical or a *diffusion bond*. In chemically-compatible coating-substrate systems, the adhesion strength can be increased by depositing films at elevated temperatures [as in chemical vapor deposition (CVD) or in physical deposition by sputtering or spraying] or by subjecting the substrate-coating composite to high temperatures after deposition. The former approach can result in a compressive state of the ceramic deposit at operating temperatures, whereas the latter may produce cracking in the deposit because of the tensile nature of the stress that will act on the ceramic coating upon heating. Elevated temperature deposition is therefore preferable to post-deposition heat treatment since ceramic materials generally behave well under a mild compressive loading.

Poor adhesion has been the biggest problem with sputtered ceramic coatings formed on beryllium substrates [2]. Sputter deposited films have also shown large deviations from stoichiometric composition and the presence of undesirable microstructures. Depending on the conditions employed during fabrication, the structure of sputtered films could be either amorphous or crystalline. Columnar growth structures with poor interparticle bonding are frequently encountered in sputter deposits.

2.5   Summary

The various types of materials and process options, as discussed above, which have been investigated at CSDL and other similar laboratories are shown in Table 2-1 [2,3,4,5]. Also listed are the options under investigation in the present body of work.

Table 2-1. Materials and process options
considered for bearing fabrication.

MATERIAL	PROCESS	PROBLEMS ENCOUNTERED
SOLID CERAMIC	SINTERING AND HOT PRESSING	DIFFICULT TO MACHINE PHYSICAL INCOMPATIBLITY LOW THERMAL EXPANSION POOR THERMAL CONDUCTIVITY
HARD COATINGS	PLASMA SPRAYING (THICK)	POROSITY, ADHESION, COHESION, PLUS ABOVE
	SPUTTERING (THIN)	ADHESION, COMPOSITION, STRUCTURE MISMATCH LESS CRITICAL BECAUSE OF COATING THINNESS
MODIFIED SURFACE	CASE HARDENING BY ALLOYING OF THE SURFACE	NONE OF THE ABOVE PERCEIVED
COMPOSITE	POWDER METALLURGY- HOT ISOSTATIC PRESSING	NONE PERCEIVED

2.6   Direction of the Present Work

The broad objective which underlies all aspects of the present effort is to establish a hard, pore-free, wear-resistant surface which is integral with the beryllium structural members, thus eliminating the adhesion problems that have been encountered in the past. In the case-hardening subtask, this is approached by treating a beryllium surface with a material with which it forms hard compounds, i.e., boron. Boron enrichment of the surface, in one process, is accomplished by reactive diffusion of a freshly formed film of boron with the underlying beryllium. In another part of the work, boron ions are forced by an electrical potential to penetrate into the beryllium surface by ion implantation, a process which is relatively immune to native oxide barriers, solubilities, and diffusion coefficients.

In a second subtask the desired hardening and wear resistance are imparted by particles of a hard ceramic phase dispersed within the beryllium matrix. Such a metal-matrix composite is produced using powder metallurgy methods.

SECTION 3.

Be-B REACTIVE DIFFUSION EXPERIMENTS

3.1 Background

The approach taken in this part of the gas bearing materials development program is to produce a well bonded layer of boride or borides of beryllium by reactive diffusion of boron on the beryllium surface. A concurrent effort is to be directed towards the study of diffusion kinetics in the Be-B system in order to understand the mechanisms related to the formation of the desired coating.

The binary alloy system Be-B contains a number of intermetallic compounds of which two boron rich compounds, BeB_6 and BeB_2, are reported to have hardness values of 2600 and 3200 KHN respectively [6,7,8]. Boron also has a high hardness value of nearly 3000 KHN. Reactive diffusion of boron on beryllium is therefore an attractive means of producing a metallurgically-bonded hard-surface coating.

3.2 Progress Prior to this Reporting Period

Initial CVD experiments were performed in a simple system which could be built quickly and inexpensively. A 1.25-inch diameter quartz tube capable of being evacuated to 10 torr pressure constituted the CVD chamber. The beryllium sample located inside the tube was heated to the desired temperature by means of an RF induction coil placed around the tube.

The CVD gas or gases were then allowed to flow through the tube at desired flow rates. The CVD gas systems used were (1) decomposition of BCl_3 by hydrogen [9] and (2) thermal decomposition of

diborane (B_2H_6) [10]. The depositions were carried out at 900°C to 1000°C. The coatings were on the order of a micrometer in thickness, and generally showed hardness values of approximately 1200 KHN. Both the colors of the coatings (rusty pink) and Auger electron spectroscopy showed that there had been chemical reaction between the Be and B, with the formation of compounds of the Be-B system. Although no positive identification of the compounds could be made, it was suspected that the compounds were beryllium-rich, based both on the Auger analysis and on the rather low hardness values that were measured. Thicker coatings were attempted, but coatings thicker than about 1 micrometer tended to crack and spall. The coatings produced were, nevertheless, considered to have potential gas bearing application even if better results could not be achieved.

The investigation of diffusion kinetics required metallurgically-bonded beryllium and boron diffusion couples. It had been demonstrated that the diffusion couples could be formed by hot isostatically pressing techniques, using solid boron pieces and beryllium powder. Solid pieces of boron available commercially are of the high temperature rhombohedral β-boron cyrstalline form. The lower temperature form, tetragonal γ-boron, is the more likely variety that would result at the temperature used for CVD on beryllium. Since γ-boron is not available commercially, some solid pieces of this boron-type were produced by the Arc Plasma Spray process using commercially available β-boron powder[11]. These were to be used for the preparation of Be-γB diffusion couples by the HIP technique that had already been investigated.

3.3   Progress During the Past Year

3.3.1   CVD

All the previous depositions were done at 900°C and higher. In order to ascertain the effects of depositions at lower temperatures, several CVD runs were made at 700° and 800°C using both the $BCl_3 + H_2$

10

and B_2H_6 gas systems. The BCl_3 + H_2 gas gave gray flaky deposits which came off quite easily. B_2H_6, however, produced highly adherent metallic gray deposits on about 75 percent of the surface areas. The deposits were uniformly continuous with the uncoated areas occurring at the peripheries of the disc-shaped samples.

To evaluate these coatings, the following analytical procedures were used: Microhardness measurements, optical microstructure examinations, Auger spectroscopy and X-ray diffraction.

The hardness values shown in Table 3-1 were the highest measured so far. Loads of 100 grams and higher in each case gave hardness values typical of the Be substrate. Hardness values increased as the loads were decreased down to 5 grams, with the maximum values occurring at the lowest load. In all cases, these were well over 2000 KHN. The CVD coating was, therefore, concluded to consist of either boron or of some boron-rich beryllium boride.

Metallographic sections of the samples were prepared by making a slanting cut which produced approximately a 10 fold amplified view of the CVD coating. In order to define the outer surface of the CVD coating, a nickel film was sputter-deposited on it prior to metallographic sectioning and polishing. Figure 3-1 shows the micrograph of such a polished section of sample No. 95 which was CVDed at 700°C for 1 hour. The coating consists of an outer metallic gray layer and a pink layer next to beryllium. In between these two layers is a thin layer which is somewhat lighter pink in color. Auger analysis showed the outermost layer to be boron. The rest of the film showed both beryllium and boron, suggesting that some borides had indeed formed. The total thickness of the film is about 3 micrometers as measured from the photomicrograph. A depth profile measurement by sputtering and simultaneous Auger scanning in the Auger machine, followed by a depth measurement of the sputtered crater by profilometry, indicated the thickness of the film was about 5 micrometers. Therefore, it appeared that the thickness throughout the coating was not uniform.

Table 3-1. Microhardness values of surfaces of Be CVDed at 700°C and 800°C using various indentation loads.

INDENTOR LOAD (gm)	MICROHARDNESS (KHN)			
	#93 700°C-30 min	#95 700°C-1 hr	#92 800°C-30 min	#94 800°C-1 hr
300	350	300	310	300
200	340	280	380	310
100	390	250	320	330
50	610	730	430	580
25	865	1395	630	1080
10	1605	2540	2600	2380
5	2200	2645	----	2590

2/81 CD22724

12

Ni

Be – B

Be

1/81 CD22539

←→| |←— 10 µm
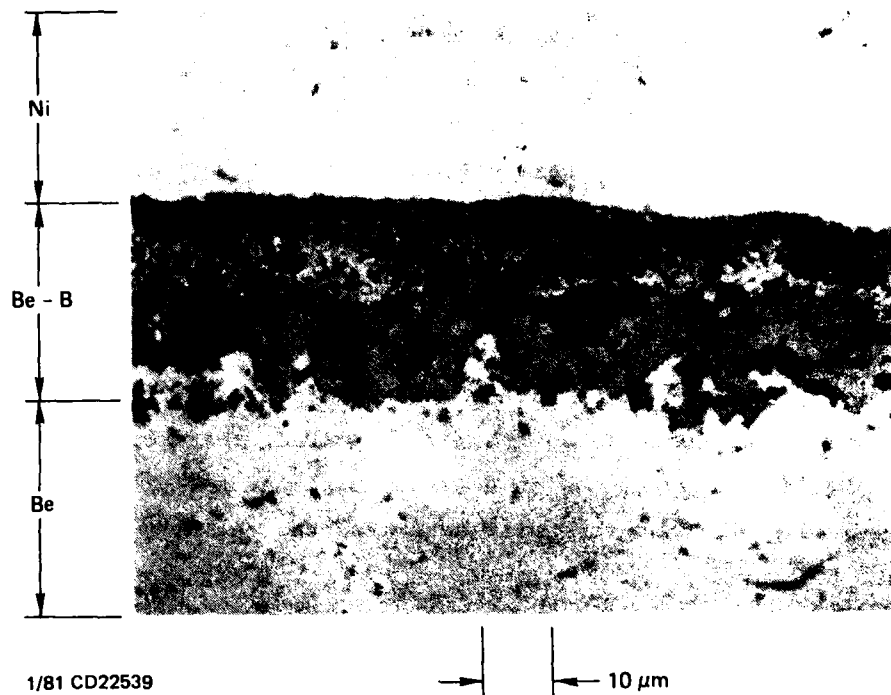
Figure 3-1. Sample number 95. Slant cut at
approximately 10:1.

13

Auger analysis of all four samples showed the outer-most layers consisting of boron with intermediate layers containing both beryllium and boron. Large amounts of oxygen were seen in areas where no coatings were formed. It was not possible, however, to obtain structural information from the Auger analysis of the samples. X-ray diffraction of the coated surfaces was, therefore, tried to obtain structure data. The diffraction patterns obtained showed peaks only representative of the beryllium substrates. It was concluded that the thickness of the films were insufficient for X-ray diffraction. The next attempt at structure determination was to try forward reflection electron diffraction. The diffraction pattern showed a few broad halos, but no Debye rings or Laue spots were seen. It appeared, therefore, that the boron deposited during the CVD on Be using diborane had produced amorphous boron. Further work will determine the validity of these structural findings.

3.3.2   New CVD System

Although the CVD films formed were of substantial thickness (up to 5 micrometers), well bonded, and with hardness values reaching 2500 KHN, the coverage of the surface was not complete. Analytical procedures indicated that presence of oxygen in the system might be responsible for this observation. It was concluded that a much cleaner CVD system should be built to succeed in producing uniformly CVD-coated beryllium surfaces for gyro gas bearings.

A new CVD system, consisting of a stainless steel bell jar, all-stainless steel plumbing, and a high vacuum pumping system equipped with a stainless steel liquid nitrogen trap was designed and built. The bell jar is capable of being baked out during evacuation and then water cooled during the CVD run. A 1-inch copper base plate is used as the bottom closure for the bell jar, through which the following functions are brought into the bell jar: screened vacuum pump port, CVD gas inlet and outlet, and RF power terminals. The RF power is supplied

14

to the system by a newly acquired 20 KW Westinghouse RF generator. The
bell jar is provided with a quartz window viewing port on the top and
another located on the side for measurement of sample temperature with
the RF coil either in a vertical or in a horizontal position. The
overall view of the system is shown in Figure 3-2. The copper base
plate with all of its attachments is shown in Figure 3-3. Because of
the large power capability of the present system, it will be possible to
use larger RF coils to produce CVD coatings on actual gas bearing
parts. The present system will also allow high vacuum type of
rotational mechanisms for sample rotation if these become necessary
during the CVD process to produce the desired uniformities of the
coatings.

3.3.3   Recent Experiments in the New CVD System

After a vacuum-bake-out the CVD chamber attained a vacuum of
about 10^{-7} torr. Be samples heated in this system either in flowing argon
or under vacuum at 800°C showed negligible surface oxidation over what
existed in the as-polished condition of these samples. Being satisfied
with the quality of the ambient atmosphere inside the CVD chamber, we have
made a number of CVD runs using diborane gas, which is composed of
99.9 percent high purity argon plus 0.1 percent diborane. After the
sample with polished surface is mounted inside the RF coil, the system is
pumped down and then given a low temperature bake-out at about 100°C for a
few hours. This produces a vacuum of 10^{-7} torr. High purity argon is
then allowed to flow at a rate of between 1 to 2 litres/minute. The
sample is now quickly raised to the preselected CVD temperature by RF
induction. Argon flow is then replaced by the argon-diborane mixture.
The film starts to form immediately and the temperature tends to decrease,
and the system requires a gradual increase in the RF power input to
maintain the temperature constant. At the end of the preselected time the
RF power is turned off and the sample is allowed to cool down quickly.
The diborane source is then shut off and the system is thoroughly purged
with pure argon before the bell jar is lifted and the coated sample is
removed.

HIGH VOLTAGE
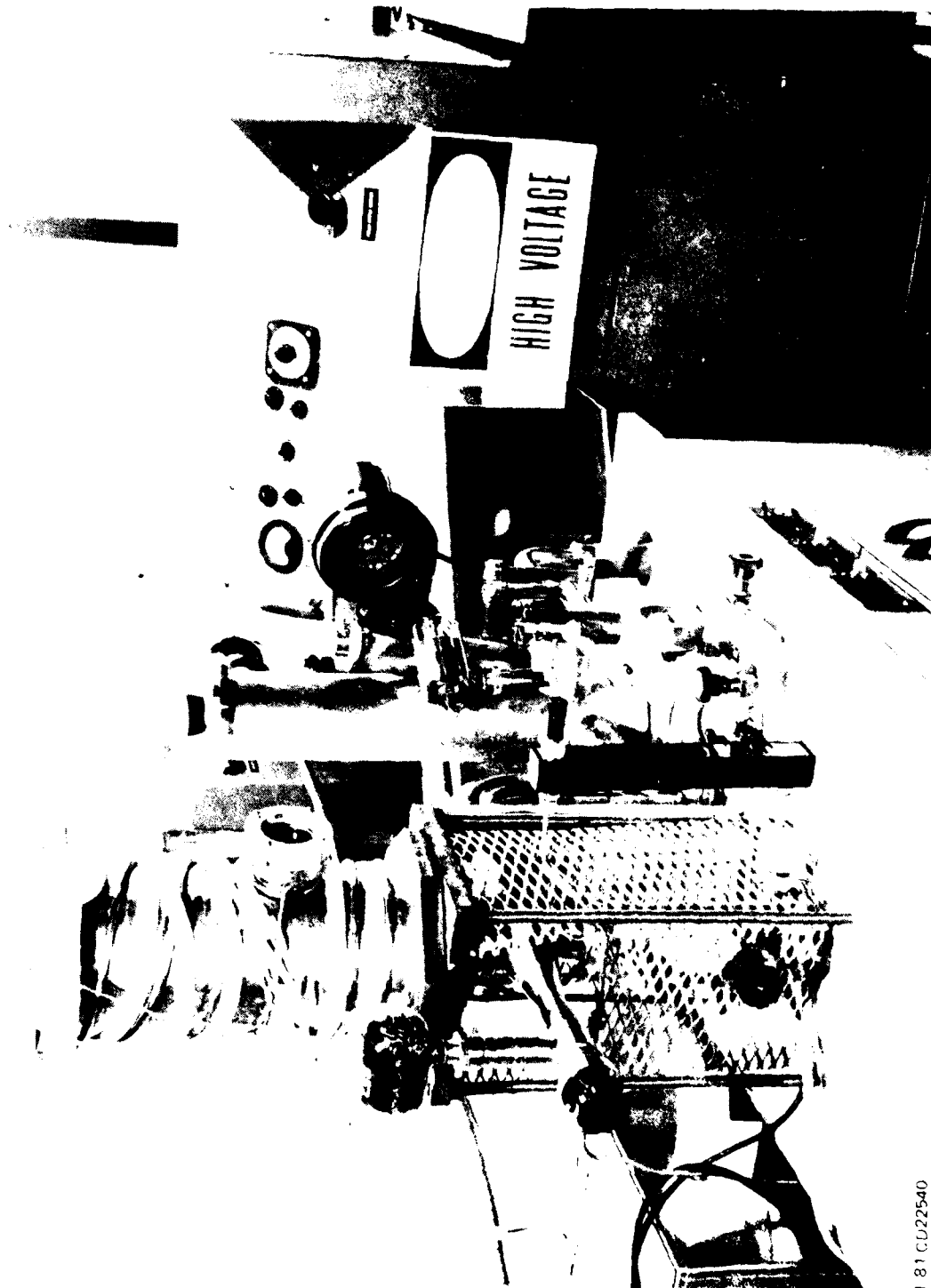
Figure 3-2. An overall view of the new CVD system. Stainless steel bell jar with necessary plumbings is located on table top. The 25 KW RF generator is located to the right of the table.

1 81 CU22540
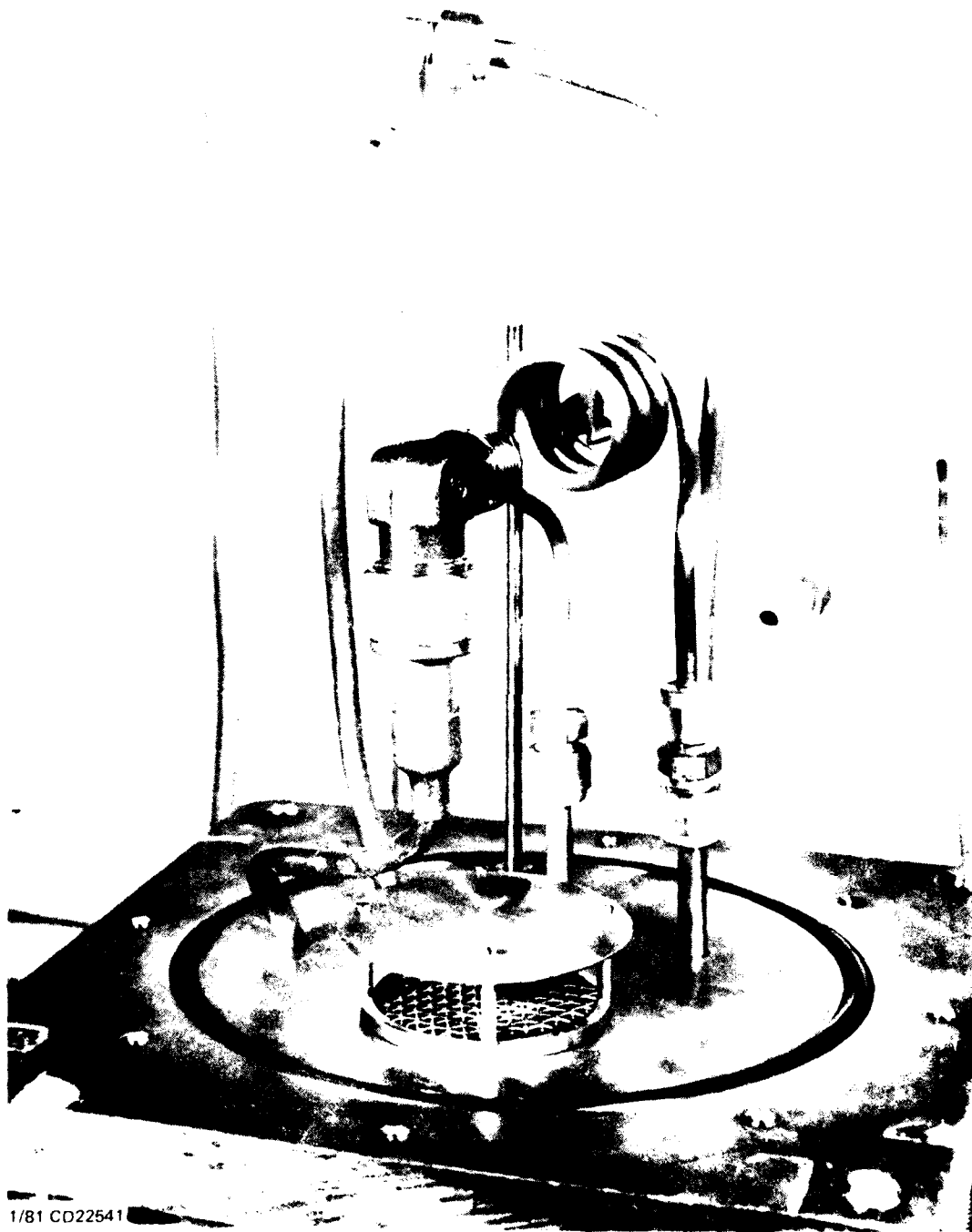
Figure 4-4. The 1-inch copper base plate of the CVD bell jar
through which RF power connections, gas inlet and
outlet and vacuum pump port are brought in.

The surface of a typical CVDed sample has a dark gray and fine granular appearance. The surface is, however, completely coated by the CVD film. The few samples produced so far at temperatures of 700°C and 800°C for various lengths of time at different gas flow rates show no sign of spalling. Figure 3-4 shows the appearance of a CVD coated sample at 500X magnification, which clearly shows the granular nature of the surface. The granular structure, however, is only superficial, as indicated by the appearance after mild polishing as shown in Figure 3-5. The coatings produced in the new CVD system not only cover the entire surfaces of the samples, they also appear to have higher hardness values compared to those prepared in the older CVD system. Table 3-2 shows the hardness values of a few preliminary samples prepared under varying time, temperature, and gas flow rate conditions.

The hardness value at 10-gram load in each case is over 3000 KHN. A comparison of samples N-16, N-17, and N-18 shows that the longer time of deposition gives higher hardness at heavier loads. A faster flow rate of the CVD gas into the chamber does not appear to have any effect. Assuming that higher hardness values under heavier indentation loads are an indication of a heavier film thickness, time at temperature is more significant than the amount of diborane gas available. When the samples N-17 and N-18 are compared, it is seen that, at heavier loads (50 and 100 grams) the hardness values are vei⋅ ⋅imilar, indicating that the thicknesses of the films are about the same at both 700°C and 800°C deposition temperatures. At low loads, however, where the intrinsic hardness of the film plays a more important role, it appears that 700°C produces a more stongly bonded deposit. At this moment it is difficult to say whether these measured differences are significant or within the limits of measurement error. A remarkable difference exists, however, between the best samples produced in the original CVD system and the cleaner new system. The hardness values of the best samples from Tables 3-1 (No. 95) and 3-2 (No. N-19) are plotted

18

20 μm
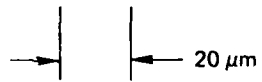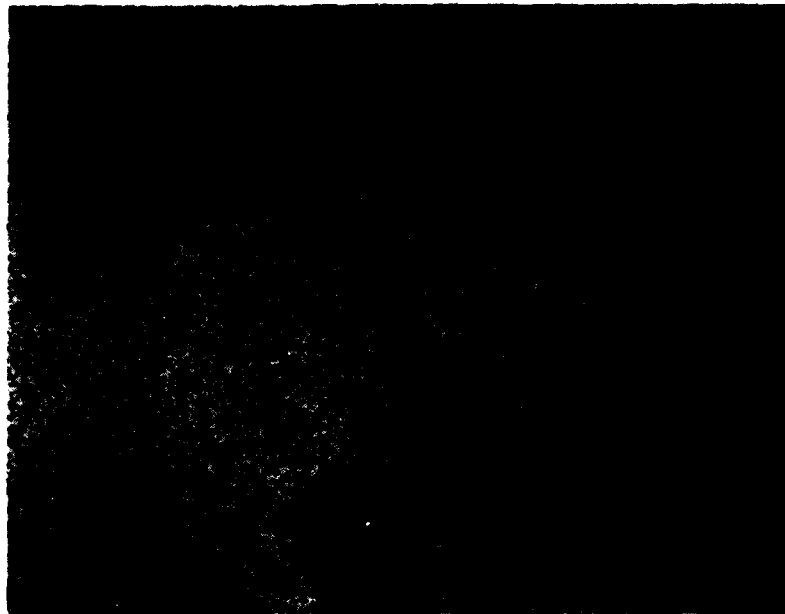
Figure 3-4. Surface of a sample CVDed at 800°C for 17 minutes. Polished w[·] h 0.3μ Al_2O_3.

1/81 CD22543

— 20 μm
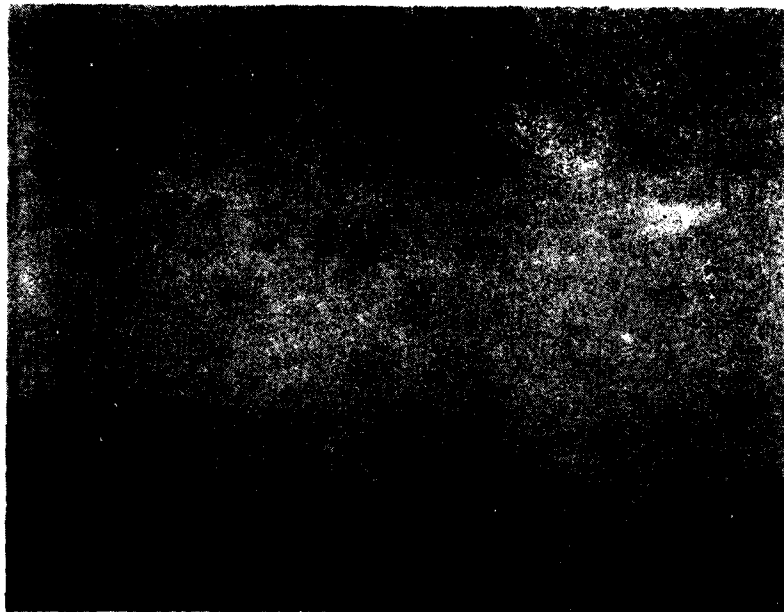
Figure 3-5. A similar sample as in Figure 3-4 after polishing the surface successively with 15 μm, 6 μm, and 3 μm diamond and 0.3μ Al_2O_3.

Table 3-2. Microhardness values of several samples prepared in the new CVD system.

INDENTOR LOAD (gm)	MICROHARDNESS (KHN)			
	#N-16 800°C-1 hr GAS FLOW-1 1/m	#N-17 800°C-2 hr GAS FLOW-1 1/m	#N-18 800°C-1 hr GAS FLOW-2 1/m	#N-19 700°C-1 hr GAS FLOW-1 1/m
300	264	329	233	445
200	305	389	240	481
100	564	923	342	945
50	1023	2148	947	2196
25	2113	3075	2282	3385
10	3286	3113	3242	3636

2/81 CD22726

21

against the indentation load (Figure 3-6) to graphically show this significant improvement in the quality of the deposits produced in the new system. The hardness values for samples prepared in the new system exceed those measured for the samples produced in the previous system substantially, measured under any indentation loads. Obviously, the coatings are now thicker and the bonding of the atoms possibly stronger.

3.4   Diffusion Studies in Be-B System:

The study of diffusion kinetics in the binary Be-B system was to be carried out using hot isostatically pressed diffusion couples. At the moment the prospect of success using this technique looks gloomy. In the last annual report the success in preparing solid pieces of γ-tetragonal boron by Arc Plasma Spraying was stated. Subsequently, there was no difficulty in producing Be-B diffusion couples by HIP technique to produce Be- γB diffusion couples. At the same time, a number of Be- βB diffusion couples were also prepared. In both cases, there were good diffusion interfaces formed between Be and B in the as-HIP condition. Such an interface between Be and γB is shown in Figure 3-7. The dark areas within the interface are believed to be pull-outs during polishing and therefore would not be a cause for concern for further diffusion heat treatments. However, diffusion heat treatments of these couples which were performed at elevated temperatures produced unexpected failures. Metallographic examination cf the interfaces showed that the beryllium had separated from the diffusion zone. This separation must have occurred at a very early stage of the diffusion heat treatment, since there is no apparent growth of the diffusion zone. An area of the interface in the Be- γB diffusion couple is shown in Figure 3-8.
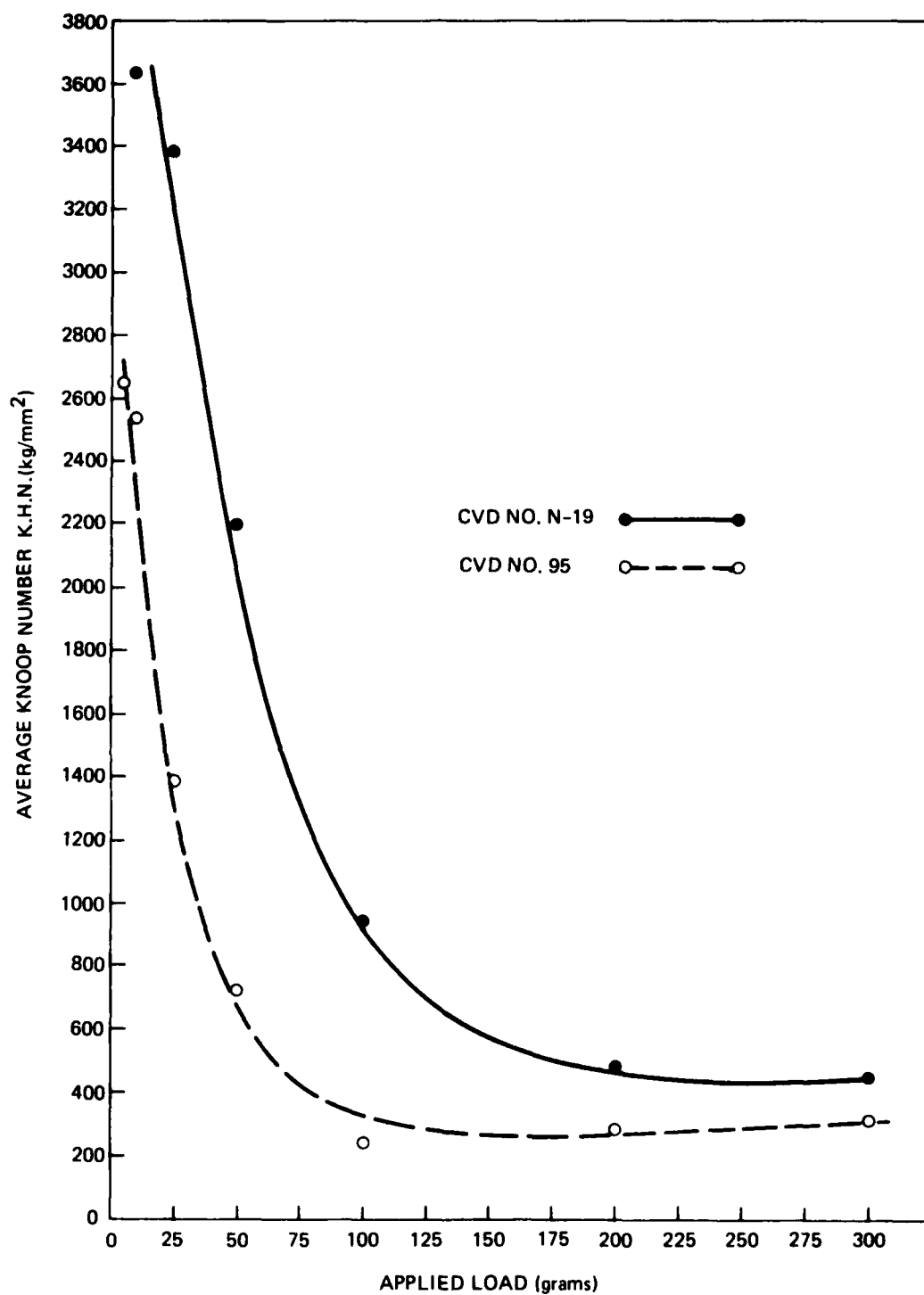
Figure 3-6. Microhardness versus indentor load. A comparison between old CVD number 95 and new CVD number N-19 shows dramatic improvement.

23
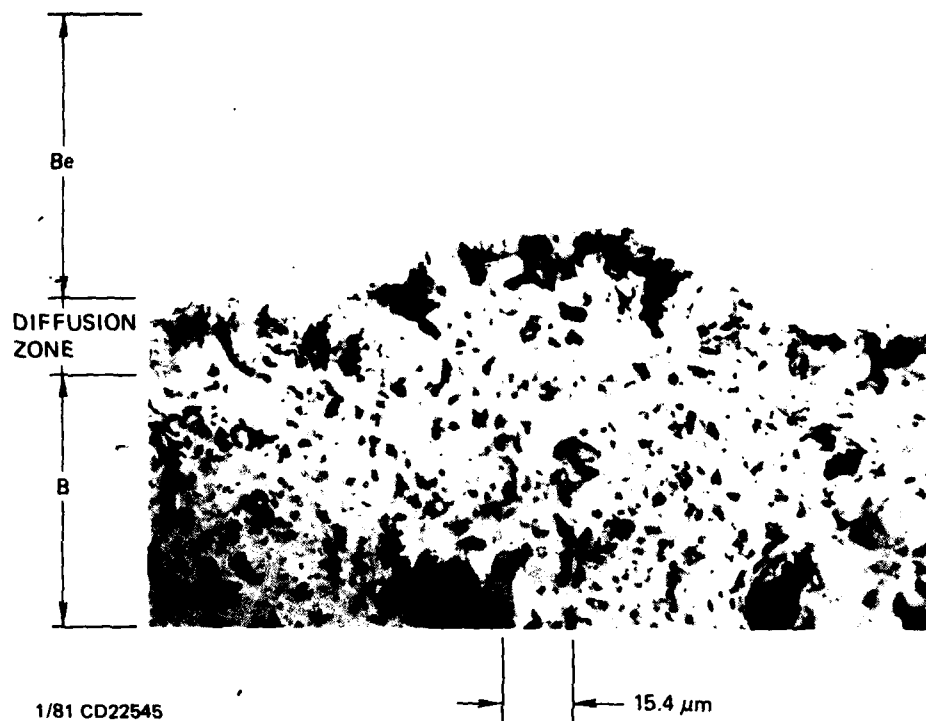
Figure 3-7. Polished interface of Be-γB diffusion couple formed by HIPing γB pieces surrounded by Be powder.
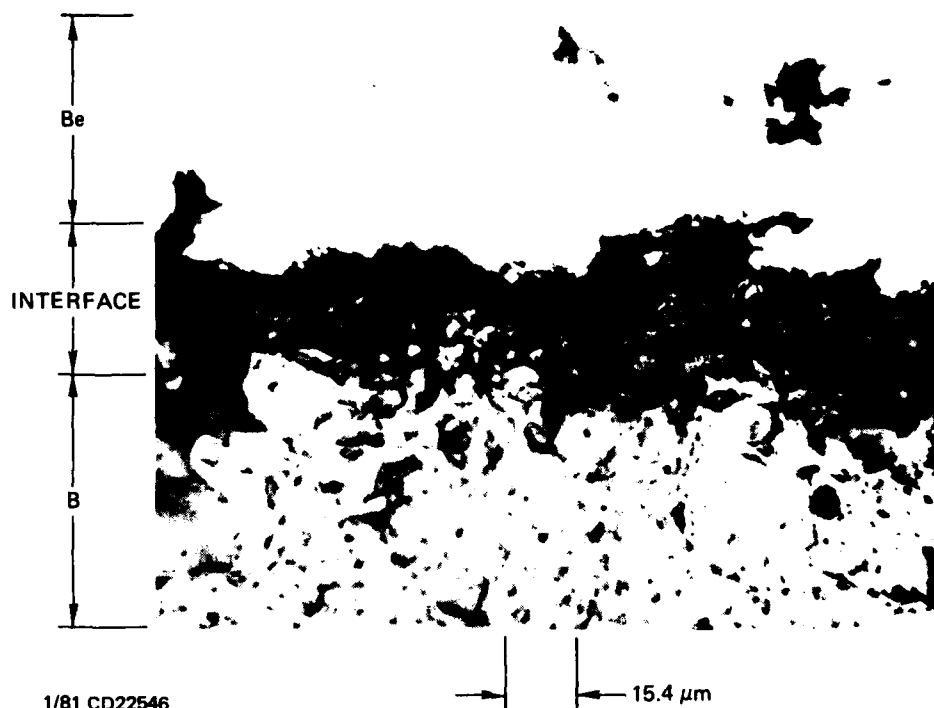
Figure 3-8. The interface between Be and B shows that Be has pulled away during the attempted diffusion heat treatment at 900°C.

3.5 CVD Samples as Potential Diffusion Couples

A very preliminary diffusion heat treatment was given to sample No. N-10 produced in our new CVD system. Sample No. N-10 was CVDed at 800°C for 1 hour at a gas flow rate of 1 litre per minute. This was further heat treated at 900°C for 6 hours in purified helium. The sample surface was boron with a metallic gray color. After the heat treatment the surface color had changed to rusty pink. An electron diffraction pattern was taken at a low glancing angle to this surface. Similar as-deposited CVD surfaces were found to be boron by Auger analysis, and electron diffraction patterns typically consisted of a couple of halos, characteristic of amorphous materials. The diffusion heat treated surfaces, however, gave non-continuous Debye patterns. The measured 'd' spacings of these rings produce a fairly good match with both the BeB_2 and the BeB_6 structures. It is believed that the upper surface layer is BeB_6 because of the color. We will try to obtain more positive verification. The electron diffraction data are shown in Table 3-3.

3.6 Discussion and Conclusions

CVD experiments using the old CVD system indicated that fairly hard coatings, diffusion bonded to the beryllium substrate, could be formed. The surface of the coating consisted of boron. Roughly 25 percent of the beryllium surface, along the periphery of the CVD film, remained uncoated. Analytical results indicated that oxygen contamination was one of the main reasons for lack of coating in these areas. The CVD system was suspected as the source of oxygen, and an extremely clean new system, essentially free of oxygen, was designed and built. This effort has now resulted in the preparation of much higher quality and highly adherent CVD deposits, with complete coverage of the surfaces.

26

Table 3-3. Electron diffraction data of diffusion heat treated sample No. N-10.

'd' - SPACING	POSSIBLE PHASES	'D' - SPACING	POSSIBLE PHASES
4.82	BeB_2, BeB_6	2.52	BeB_2, BeB_6
4.10	BeB_2, BeB_6	2.28	BeB_2, BeB_6
3.04	Be_2B, Be_4B	1.47	Be_2B
2.60	Be_6B		

2/81 CD22727

The initial objective was to produce a diffusion bonded, high hardness film of either BeB_2 or BeB_6. However, diffusion bonded coatings of amorphous boron, which may be just as wear resistant and also possess a low friction coefficient for gas bearing application, have been produced by CVD. The preliminary heat treatment further appears to have converted the as-deposited film to BeB_6. Further heat treatment at higher temperature and/or longer time may allow diffusion to proceed further with the formation of BeB_2. It is believed that the initial objectives have been achieved. Further scientific and engineering studies are needed and will continue.

As for the studies to determine the diffusion kinetics, the conventional technique of diffusion couples with infinite sources of both the elements Be and B seems to have very little prospect of success. However, meaningful results with CVD samples in this area appears promising. Although beryllium would still be an infinite

27

source, boron being of the order of a few microns would provide a very finite source of the element. Nevertheless, studies to determine the diffusion kinetics must continue with the CVD samples, which would provide important scientific information for engineering applications.

3.7   Future Plans

Efforts will be concentrated:

(1)   To further studies of the CVD process at 700°C and 800°C, as well as the investigations at higher temperatures.

(2)   To characterize the CVD films formed at various temperatures with respect to chemistry, structure, thickness, and hardness.

(3)   To study diffusion characteristics of the CVD coatings, and obtain limited diffusion kinetics results.

(4)   To produce coatings with outer surfaces of boron, BeB_6, and, if possible, BeB_2.

(5)   To determine wear and friction characteristics of the different surface structures produced.

SECTION 4.

ION IMPLANTATION

4.1   Background

As a metallurgical coating process, the use of ion implantation
for case hardening or surface alloying is an emerging technology [12],
even though it is fully mature as a manufacturing method for semi-
conductor electronic devices. The technology transfer is not straight-
forward, however. Ion implantation in semiconductor processing intro-
duces only minute quantities (doses) of foreign atomic species (dopants)
which are intended to alter only the electronic characteristics of a
shallow region in the surface of a substrate. Metallurgical modifica-
tion of materials, on the other hand, implies the use of massive doses
of the alloying agent to produce compositional changes, including the
formation of new phases or distinctive solid solutions. Much of the
current effort is thus necessarily exploratory in nature, not only in
assessing results but also in developing processing and testing
procedures.

The ion implantation process differs from those based on
diffusion by employing kinetic rather than thermal energy to introduce
and emplace the foreign species which is intended to modify the host
material. A high kinetic energy is given to the species to be
implanted, such as boron, by first inducing ionization and then
accelerating the ions through an electrical potential difference. They
are then directed as a beam or current of ions onto a substrate
material, such as

beryllium, whose surface their high kinetic energy allows them to pene-
trate. The quantity or dose of boron delivered is determined by the
magnitude of the current and the length of time it is applied. The
range of penetration of the ions depends on the accelerating poten-
tial. Consequently, for ion implantation processing the concentration
of boron in the surface of the beryllium is not limited by its
solubility, and the penetration of boron into the beryllium is not
restricted either by the diffusivity of the boron or by the presence of
a native oxide film on the beryllium. However, these characteristics
are limiting factors in the more conventional boriding processes.

From the foregoing, it can be seen that a major feature of ion
implantation is the control which it affords - control of quantity
through control of both dose-rate (i.e., ion current) and deposition
time, and control of penetration depth through adjustment of the
acceleration voltage. By selection of appropriate combinations of dose
and accelerating voltage, unique concentration profiles of dopant with
depth can be attained, some of which could never result from the action
of the natural laws governing solid-state diffusion. Other features are
the control of lateral distribution of concentration through rastering
or masking off of the ion beam, precise selection (purity) of the
element to be implanted, and a clean high-vacuum environment protecting
the surface undergoing treatment.

4.2   Previous Work

4.2.1   Experimental Objectives

It was pointed out previously that the large body of accumu-
lated experience in the ion implantation of semiconductors is only
partially applicable to this program. Evaluation of boron implantation
as a method of making beryllium surfaces usable directly in gas bearings
required answers to questions such as the following:

(1) The feasibility of implanting metallurgically significant
    quantities of boron in reasonable time periods using
    present-day equipment.

(2) The compatibility of the sputter erosion rate of beryllium
    in a beam of boron ions (since sputtering to a greater or
    lesser extent inevitably accompanies implantation) [13]
    with (a) retention of precise physical dimensions and good
    surface finish and (b) build-up of a high concentration of
    boron in a beryllium substrate.

(3) The possible need for post-implant heat treatment to
    enhance the hardness and wear resistance of the implanted
    surface.

(4) The formation of specific identifiable beryllium-boron
    compounds as a result of implantation and/or heat
    treatment, and the kinetics of their formation.

Experimentation to answer these questions began with the
equipment and materials at hand, in full recognition that these were
less than optimum. The results obtained through the end of the last
reporting period have been discussed [14,15] earlier and are summarized
here.

4.2.2   Summary of Results

The first few small samples of beryllium implanted with boron
were prepared at the Naval Research Laboratory in a low current machine
so that the processing time requirement was inordinately long, but they
sufficed to show that significant boron concentrations could be attained
in beryllium surfaces. Two independent methods of assessing erosion due
to sputtering indicated that it was negligible and therefore did not set
any serious limits on the concentrations which might be reached.

31

In this phase, the specimens prepared were calculated to contain 10, 20 and 40 atomic percent boron uniformly distributed within a layer 0.8 μm deep. Hardening, as tested with a Knoop indenter, occurred upon implantation and increased further with heat treatment; the hardness increase on heating was considered to be an indication that the initial hardening was a result of compound or quasi-compound formation and not primarily due to lattice strains stemming from the intrusion of a foreign species. This interpretation was also consistent with Rutherford back-scattering measurements done on some of these samples at the Naval Research Laboratory (NRL).

A second group of specimens, of a size (3/4-inch diameter) large enough to permit friction and wear testing after implantation, were next processed in a new implanter whose higher current capability made it a credible metallurgical tool. These were implanted to levels of 60 and 40 atomic percent B in Be and again showed hardness increases. However, inconsistencies and a lack of reproducibility showed up the need for more than a single sample of a given type. Improved effectiveness in heat dissipation during the 40 atomic percent implantation may have been the main reason for the much better surface finish observed on the 40 atomic percent as compared to the 60 atomic percent 3/4-inch sample.

4.3   Uniform Concentration vs. Graded Concentration
         Layers

The first phase of the work done with boron implants in beryllium made use of energies (i.e., accelerating voltages) ranging from the lowest usable value to the highest voltage attainable. The quantity of boron implanted at each voltage was adjusted so that collectively they would result in a uniform concentration of boron throughout a layer extending to a depth of about 8000 A, or 0.8 μm. From that depth the concentration was predicted to "tail off," following a Gaussian distribution into the bulk of the beryllium as it would for a single monoenergetic implant.

32

A more efficient use of implanter time, as well as a tougher
and more effective wear surface, should result from a different
combination of parameters for the implantation schedule. The objective
is to have the boron concentration heaviest at the surface of the
implanted substrate and decreasing in an approximately linear profile
with depth. Hardness would thus be highest at the surface, where it is
needed to provide wear resistance, and the smooth decrease in hardness
(and concomitant increase in ductility) with depth would tend to safely
dissipate stresses applied to the wear surface. This should mitigate
any tendency, should it exist, of a hard, brittle layer to separate from
the bulk material at an interface where properties undergo an essen-
tially discontinuous change.

The implantation schedule to produce a graded layer would call
for high doses at low energies to impregnate the surface, followed by
progressively lower doses at the higher energies affecting the deeper
levels of the subsurface. The greater economy in usage of machine time
is apparent when it is considered that the generation of uniform
concentration layers has required progressively heavier doses, and
therefore longer exposure times, at the higher energies.

Emplacing all of the boron by way of selected combinations of
implants is one possible way of attaining graded layers, but an
alternative method could be equally or perhaps even more economical in
its demands on implanter time. That alternative would be to cover the
surface to be hardened with a thin film of boron and then implant
through the film with high energy boron ions. Several processes would
be expected to act on the boron in the film to move it into the
beryllium: ion mixing, knock-on or recoil implantation, and radiation-
enhanced diffusion. These concepts have been demonstrated and discussed
in the literature [16], but the idea of using a high-energy implant to
redistribute a film or surface layer of the same element has not been
reported.

A cardinal feature of this portion of the program was to prepare samples of graded concentration implants by both methods and study them in comparison with the uniform concentration layers prepared in the first phase of the work.

4.4   Methods of Examination

Examination and comparison of implanted specimens was proposed to be carried out using a variety of measurement and analytical techniques. Among these were the following:

(1)   Microscopic examination

(2)   Microhardness testing

(3)   Friction and wear testing

(4)   Electron diffraction

(5)   Surface profilometry

(6)   Rutherford back scattering

Optical microscopy, including Nomarski differential interference contrast to accentuate topographical variations, was intended to reveal changes in surface finish resulting from the implantation process. Microscopy, or more specifically photomicrography, also enters into the micro-hardness testing through its use in measurement of the length of the imprint of a diamond pyramidal indenter.

Of the two common types, it is the Knoop indenter which is used here because its shallower penetration affords a better chance to derive meaningful data from the very thin surface layers which result from implantation. More will be said on this subject later.

Measurement of friction coefficient versus a standard material can be regarded as another way of characterizing surfaces and differentiating between the results of various treatments. Aside from that, friction and wear testing in this program has obvious practical

34

value in indicating the relative merit of differently treated beryllium surfaces for gas-bearing service. There are a number of accepted testing methods for friction and wear [17,18] -- the procedure used here is the pin-on-disc method. This allows a single implanted disc to be tested after each of several treatments (e.g., before and after heat treatment) while still retaining a substantial portion of the surface undisturbed and usable for hardness testing, Auger analysis, profilometry, or electron diffraction.

Initial friction and wear testing in this part of the program was done with pins of a material commonly used for this purpose, i.e., 52-100 steel. The tests were performed on freshly cleaned surfaces without lubricants or coolants, as a means of ensuring well defined and reproducible conditions. Perhaps because of the absence of any lubricating film, in many instances the steel pin material "crayoned" itself onto the disc surfaces resulting eventually in steel rubbing on steel. This occurence, plus the desire to generate data with more direct engineering value, led to a redesign of the test apparatus to include an aluminum oxide (sapphire) tipped pin. Friction and wear data reported in future periods will include performance of implanted surfaces against this harder stylus material.

During this reporting period, friction and wear testing was performed on uniform layer samples which had been implanted, and whose hardness increases had been reported, in the previous period. The compilation of wear test results below also includes data from the earliest of the graded layer structures which comprise the major effort in the present phase of the program.

One of the objectives of this program of research was to determine which, if any, of the hard compounds in the beryllium-boron system could be made to form within the surface. This is especially hard to predict for a materials system put together by ion implantation, since it is not governed by the conventional laws of chemical thermodynamics or kinetics. Of course, once the bo on is in place

within the beryllium structure, these laws will be operative but many of the pertinent parameters, such as the nature and concentrations of the many defects induced during implantation, are not known.

The proposed method of detecting and characterizing beryllium boride compounds was by transmission electron microscopy (TEM) and diffraction. Samples for this study were to be prepared by first coring out a small (3mm) cylinder from the appropriate disc by electrical discharge machining (EDM). The implanted surface was then to be sliced off and the resulting disc thinned, first by abrasive removal of the unaffected beryllium from the underside and then by jet thinning in an electro-chemical procedure. This was seen as permitting the sampling and study of the implanted discs at various stages in their treatment.

Complications not foreseen were:

(1) The relatively low survival rate of TEM samples during their preparation for examination (yields are usually about 30 to 40 percent), and

(2) The conventional practice of electro-thinning from both sides of the specimen.

These considerations prevented the satisfactory collection of data as originally planned. First, although the area toward the center of the 3/4-inch sample disc was "reserved" for TEM coring and hardness measurements, that region within the smallest proposed wear track (1/2-inch diameter) was capable of furnishing only two or three cores altogether so that taking several samples at any given stage of treatment was an unsupportable luxury. The procedure of thinning from both sides also was not compatible with the study of layers at, or very near, one surface, particularly when the precise level, at which the material in the disc would be revealed to the electron beam, was not known or controllable.

36

A search for an alternative means of studying structures led to consideration of reflection electron diffraction (RED). After some scrutiny of the problem, proper fixturing and procedures were worked out to permit electron diffraction of whole 3/4-inch diameter specimen discs. There are several advantages to this, not the least of which is the absence of risk in taking and preparing samples (in contrast to the situation with TEM).

Surface profilometry was to be performed using a Sloan "DekTak" which has the very valuable feature of allowing the test surface actually under the stylus to be monitored with a low power microscope. Among other things, it is therefore possible to know exactly when any given wear track is undergoing profiling. The end product is a strip chart representation of the surface with the irregularities highly magnified.

There were two purposes for the surface profilometry. The first was to allow comparison of the sample surface before and after implantation and/or heat treatment to note any resulting changes. The second was to quantify, by recording the shape of a wear track, the friction-produced erosion of a wear-test sample surface. The cross-sectional groove area determined by profilometry can be multiplied by the length of the wear track to yield an estimate of the volume of material removed and thus a number indicating the relative wear.

Rutherford back-scattering (RBS) was to be performed at the Naval Research Laboratory for this program. In this technique, a mono-energetic beam of ions (commonly helium ions, or alpha particles) is directed onto a test specimen and the energy spectrum of the back-scattered ions is recorded and analyzed. Energy losses indicate the elemental species present and to some extent show the depth and distribution of these species within a sample.

4.5   Status of Current Work

4.5.1   Sample Preparation

The first samples implanted in this gas bearing materials study
were I-400 grade beryllium from an unknown vintage, with surfaces
prepared by careful hand lapping and polishing. Subsequently, a wider
ranging and more precisely controlled program of testing was undertaken,
and the need for better definition and control of parameters, including
substrate composition and condition was evident. Accordingly, all
the discs intended for wear testing, with sufficient area for other
studies, were cut from a particular lot (Brush Wellman #4784) of I-400
grade Be and a chemical analysis was obtained from the vendor. These
were machine lapped to a good flatness and then carefully hand-polished
before implantation. This set of discs was used for high concentration
uniform implants, the sputter erosion question having been settled,
starting at 60 atomic percent and working downward. The series ended at
40 atomic percent when several things became apparent, among them: 1)
accurate microhardness indentation measurements and 2) accurate surface
profilometry both demanded extremely good surface finish, freedom from
scratches, and superior flatness. With the beginning of the work on
graded coatings, it was proposed to allow sufficient time and money for
increased attention to sample surface finish.

Arrangements were made for a large group of discs to be cut
from the same lot of beryllium as before and to be lapped and polished
at an organization (Applied Optics Center Corporation) which is well
established in the field of beryllium mirror polishing. This was only
partially successful because only a few discs in the first shipment were
acceptable. The difficulty was traced to an omission of a special
stress relieving heat-treatment between sample machining and the
lapping/polishing operation. This omission was corrected and the
balance of the starting material was furnished to us as adequately
polished discs, which will serve as substrates for the majority of the
work to be performed in the next reporting period.

In the interim, some implantation and coating work had already been carried out on the discs which had been accepted as having adequate surface finish. Since the discs in the first shipment had no stress-relieving heat treatment, the results from their tests will have to be viewed with some reservations and interpreted cautiously to avoid erroneous conclusions.

4.5.2 Implantations Performed

The beryllium-boron implants carried out during the period of this report were primarily intended to produce graded concentrations, both by way of successive implantations and by implanting through a precoat of sputter-deposited boron. Even so, it was recognized that some additional uniform concentration samples would also be required. One of these was a repeat of the 60 atomic percent sample which was cited earlier [15] because it had exhibited very strange surface manifestations and an unexpected RBS spectrum. Another reason for repeating uniform concentration implants was for purposes of correlation since the NRL implanter, its vacuum system, and the sample holders were continuously being "debugged" and improved. Two results of these changes at NRL were better temperature control and a better vacuum environment for later specimens as compared to those done earlier.

A wide range of surface concentrations, i.e., 10, 20, 40, and 60 atomic percent had been proposed for study in this phase of the program, but it soon became apparent that such a workload was unrealistic in terms of the time available on NRL's implanter. Because the 40 atomic percent uniform concentration gave the best friction and wear results, as discussed below, it was decided to restrict the targeted surface concentrations to that one value. As another response to the limited machine time at NRL, a second source, the SPIRE Corporation in Bedford, Mass., was developed.

Investigations of graded concentration implants was planned to take place in two steps; first the high dose/low energy (Hi/Lo) implant and then low dose/high energy (Lo/Hi) treatment. Samples were to be tested between these two phases to separately evaluate their effects. The implantations prepared during this period are included in Table 4-1, which presents all of the significant samples of current interest.

4.5.3   Microscopy/Profilometry

Microscopy and profilometry are discussed together here since they are complementary techniques for studying surface topography. Figure 4-1 shows representative areas of several of the samples prepared at NRL and at SPIRE. All optical magnifications are 500X as is the horizontal magnification for the DEKTAK trace. The vertical magnification for all DEKTAK traces is 100 times greater or 50,000X. For comparison, unimplanted beryllium, as polished, and a conventional gas bearing material, plasma-sprayed aluminum oxide, are also shown. (This Al_2O_3 surface is smoother and more pore-free than most production material, however.)

The effect of ion implantation on surface appearance and profile is clearly evident. All implanted samples are altered to some extent, although for 40-III the change in appearance is minimal and the profile is indistinguishable from the starting material.

The importance of temperature control during implantation is the most obvious observation. For the sample which shows the greatest surface disruption, 60-I, there had been essentially no cooling provided and the disc may have reached 400-500°C. It is known that it did not reach incandescence, but not much more can be said. The two samples 60-II and 40-I were implanted using an improved holder which provided a definite, though imperfect, thermal path and included a thermocouple

Table 4-1. Implanted 3/4" disc samples.

Sample Designation	Where Implanted	Nominal Peak Concentration*	Type	Heat Sinking	Remarks
60-I	NRL	60%	Uniform	Poor	First sample of this format. Four doses, 95-250 Kev
60-II	NRL	60%	Uniform	Fair	Repeat of 60-I
40-I	NRL	40%	Uniform	Fair	Four doses, 95-250 Kev
40-II	NRL	40%	Uniform	Good	Six doses, 25-192 Kev
40-III	NRL	40%	High dose Low energy	Good	Single dose, 25 Kev
40-SC-I	NRL	40%	Hybrid	Good	Single dose, 60 Kev through 1000 Å sputtered boron film
40-SC-II	NRL	40%	Hybrid	Good	Single dose, 60 Kev through 1200 Å sputtered boron film
SPIRE Hi/Lo	SPIRE	40%	Graded	Poor	Single dose, 50 Kev
SPIRE Hi/Lo-Lo/Hi	SPIRE	40%	Graded	Poor	Two doses - First as for SPIRE Hi/Lo, then one @ 200 Kev

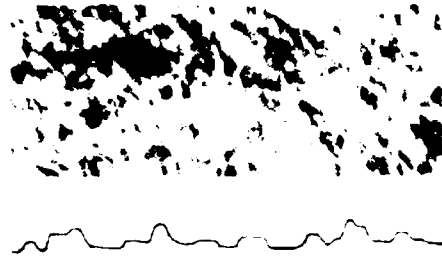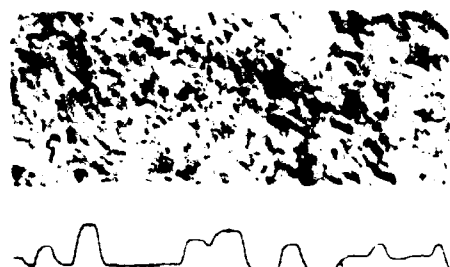* Concentrations are atomic percentages.
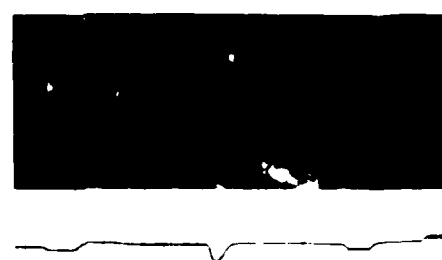
41
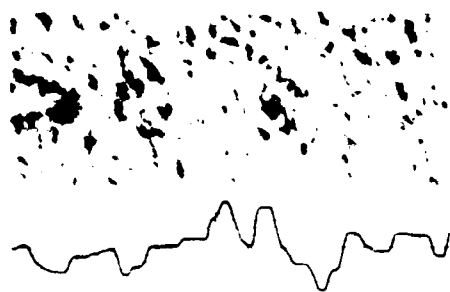
60 I 60 II

40 I 40 II

SPIRE Hi/Lo 40 III

UNIMPLANTED Be PLASMA SPRAYED Al_2O_3

2/81 CD22585

Figure 4-1. Surface appearance and profiles.

42

located several centimeters from the sample. Temperatures attained by
these samples have been estimated at 200-300°C. The latest sample
holder, used in the implantation of 40-II and 40-III, features a more
effective heat path including an underlying disc of indium foil as a
conformable thermal contact material. Although here again the
thermocouple was not in direct contact with the sample, the fact that
the indium remained unmelted shows that the sample temperature was less
than 156°C.

Cooling conditions for the SPIRE Hi-Lo implant were much
different from those in NRL and certainly less effective than for its
nearest equivalent, 40-III. Appearance and profile of the SPIRE sample
underscore the need for temperature control during implantation.

Observations of surface film color are not unique indicators of
peak temperature, resulting rather from a combination of heating and
imperfect vacuum. A blue film, assumed to be bec, was seen on 60-I and
on SPIRE Hi-Lo, while samples 60-II and 40-I had only a slight tinge of
color. On the other hand, 40-III is indistinguishable in color from the
starting material.

4.2.4   Hardness Testing

Results of pre- and post-hardness indentations are given in Table
4-2 and are plotted graphically in Figures 4-2 and 4-3. (Two graphical
displays are shown since a single plot would be too crowded to be
useful.

In the first phase of the program, great significance was
attached to the hardness measurements made on implanted surfaces before
and after heat treatment. It is still believed that these measurements
indicate that beryllium surfaces would be improved for gas
bearing service by means of boron implantation, and that the further
hardening on heat treatment is an important observation. However, it
is not asserted that the hardness operates in a linear measurement

Table 4-2. Knoop hardness readings, boron implanted beryllium.

Load, Grams	Be, I-400	60-I (uniform)	60-II (uniform)	40-I (uniform)	40-II (uniform)	40-III (Hi/Lo)	40-SC-I (Boron Coat)	40-SC-II (Boron Coat)	SPIRE Hi/Lo	SPIRE Hi/Lo-Lo/HI
50	470	395	400	410	345	345	490	340	395	460
25	510	620	550	420	480	430	620	400	430	630
10	560	800	1040	990	730	580	940	580	725	880
5	710	1450	1600	1770	980	520	1600	670	590	1580

44

Figure 4-2. Knoop hardness reading versus load
(I-100 Be with boron implantation).
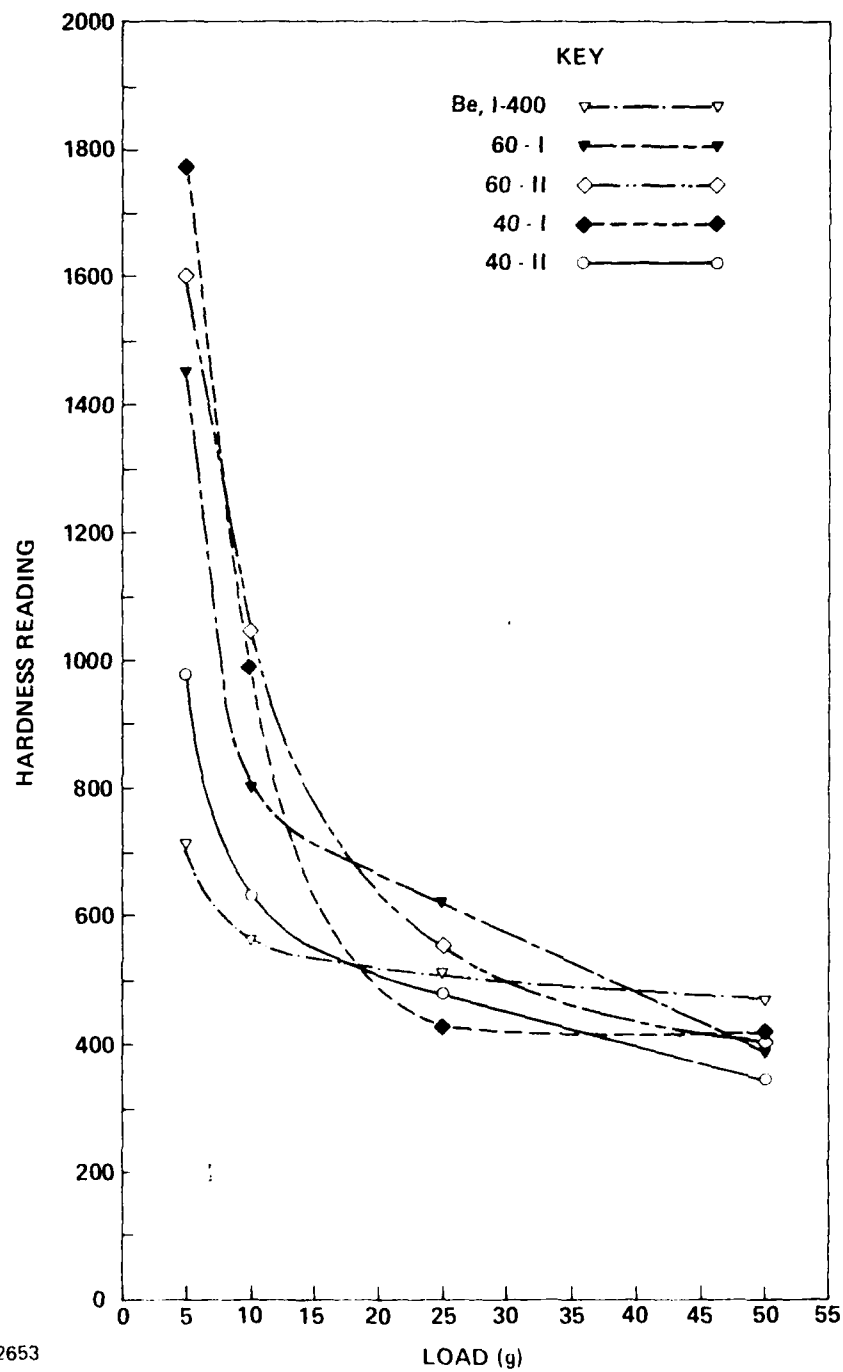
2/81 CD22653

Figure 4-3. Knoop hardness reading versus load
(I-400 Be with boron implantation).

2/81 CD22654

46

of indented imprints in these surfaces are Knoop Hardness Numbers which accurately characterize the surface layers.

There are three reasons for the reservations expressed above. First, there is the basic rule in microhardness measurement that surface layers can be tested accurately only when the layer thickness is ten times the depth of the indenter penetration into the material; otherwise the anvil effect is a source of error.[19] The minimum thickness which can be tested accurately depends on both the hardness of the material and the load on the indenter. These have been calculated for the various hardnesses and loads likely to be of interest here, and the results are given in Table 4-3. They are shown plotted in Figure 4-4, which also indicates the maximum depth, 0.8 µm. to which a uniform implant should extend under the conditions used in this program. Obviously, that depth is generally much less than is required to yield an accurate measurement.

The second factor is the difficulty in making accurate linear measurements of imprints which are only a few microns long where the surface is not absolutely flat and featureless. For example, with a 5 gram load a 6 micron imprint indicates a KHN of 1976 while a 5 micron imprint means a KHN of 2846, or 44 percent greater. Measurement of such small dimensions with three significant figure accuracy is very challenging under the most favorable conditions.

Thirdly, there is the complication mentioned above under the topic of sample preparation wherein the lack of a stress-relieving heat treatment was mentioned. All of the samples which are far enough along in their processing to appear in this report were affected by that omission.

The reservations expressed above concerning accuracy notwithstanding, it is nevertheless considered to be useful to make microhardness indentations and record them for the various samples during their processing. If the results are viewed in the proper perspective, they do have significance on a relative basis and may prove to have value in predicting gas bearing surface behavior.

47

Table 4-3. Minimum film thickness for accurate
Knoop hardness measurement.

KHN	LOAD grams	OBSERVABLE INDENTATION LENGTH	MINIMUM FILM THICKNESS
4000	50	13.24 μ m	4.45 μ m
	10	5.96	1.99
	5	4.22	1.41
	1	1.89	0.629
3000	50	15.40	5.13
	10	6.89	2.30
	5	4.87	.62
	1	2.18	0.72
2000	50	18.86	6.29
	10	8.43	2.81
	5	5.96	1.99
	1	2.67	0.88
1500	50	21.78	7.26
	10	9.74	3.25
	5	6.89	2.30
	1	3.08	1.02
1000	50	26.67	8.89
	10	11.93	3.98
	5	8.43	2.81
	1	3.77	1.25
500	10	16.87	5.62
	5	11.92	3.976
	1	5.33	1.77

Figure 4-4. Minimum film thickness for accurate Knoop hardness measurement.

4.5.5   Friction and Wear Testing

Friction and wear tests probably have the most direct relevance
to eventual gas bearing performance of any of the testing carried out
here, but the original intent of this testing was as a screening
procedure, i.e., as an indicator of relative value. For this reason,
the pin material was chosen to be the commonly-used 52-100 steel
hardened to Rockwell 63-C (800 Knoop).

Conditions chosen for the testing were approximately those
which might be found in a conventional gyroscope wheel upon touchdown:
50 grams dead-weight loading and 100 rpm. For a wear track diameter of
approximately 0.50", this corresponds to a linear speed of 400 cm/min.
Both pin and disc were solvent cleaned to arrive at a reproducible,
lubricant-free state. This condition is an extreme "worst case" in view
of the general practice of providing at least a monolayer of lubricant
in operating devices.

Results of the friction and wear testing are listed in
Table 4-4. For reference, the table includes test results for an Al_2O_3
surface, since this is a commonly used gas bearing material, as well as
the results for untreated beryllium. Samples 40-II and 40-III were not
received in time to be included here.

The friction coefficients given are straightforward in their
interpretation, except for the samples where material accumulated on the
wear track, a condition which is designated as "pick-up." This material
was determined to be iron or iron oxide, presumably from the steel
pin. It is therefore not surprising to see coefficients of friction for
those cases rising to values of 0.8 - 0.9 as they would in a test of
steel-on-steel.

50

1/81 CD22547

Figure 4-4. Minimum film thickness for accurate Knoop
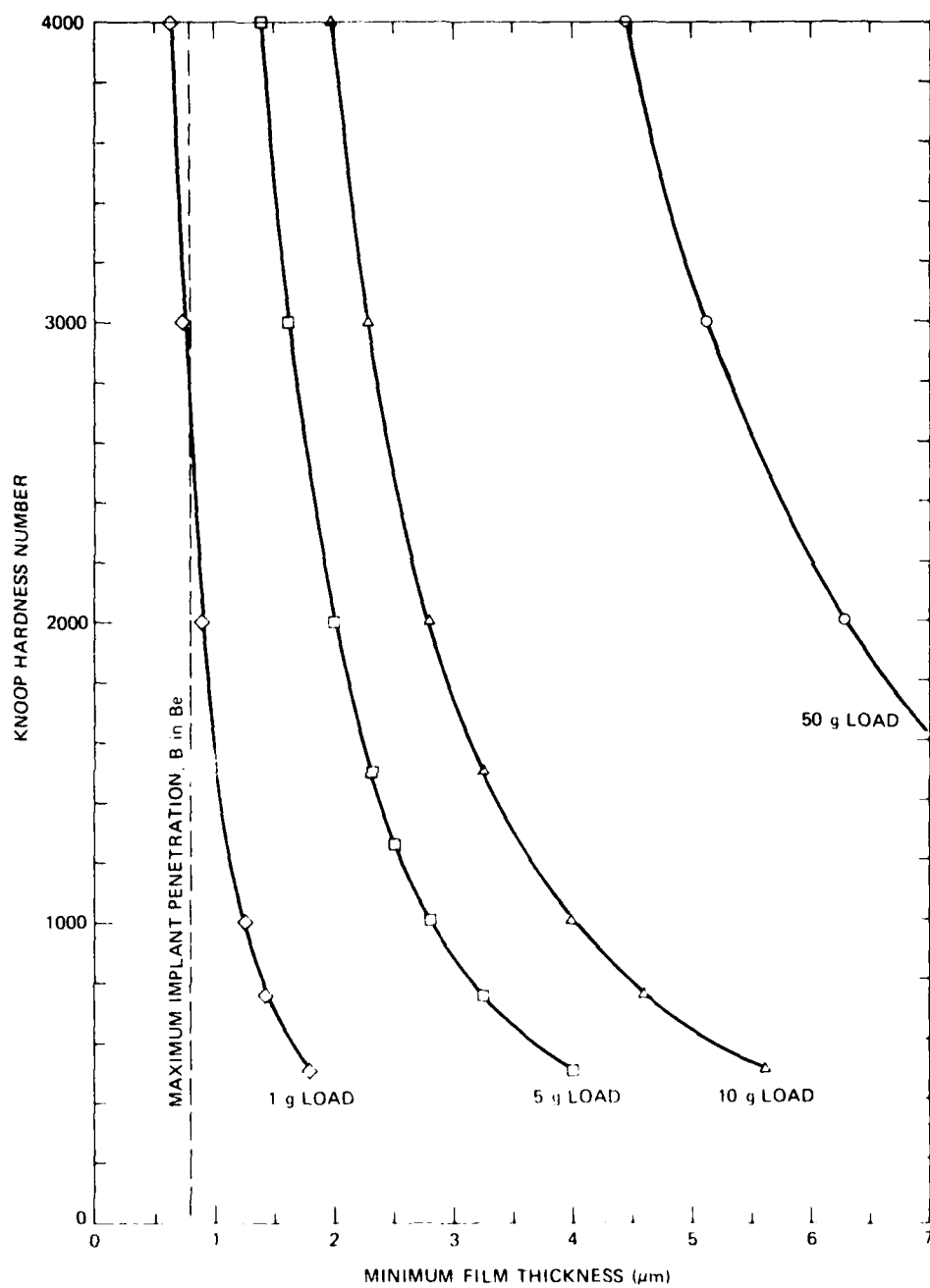hardness measurement.

49

4.5.5 Friction and Wear Testing

Friction and wear tests probably have the most direct relevance
to eventual gas bearing performance of any of the testing carried out
here, but the original intent of this testing was as a screening
procedure, i.e., as an indicator of relative value. For this reason,
the pin material was chosen to be the commonly-used 52-100 steel
hardened to Rockwell 63-C (800 Knoop).

Conditions chosen for the testing were approximately those
which might be found in a conventional gyroscope wheel upon touchdown:
50 grams dead-weight loading and 100 rpm. For a wear track diameter of
approximately 0.50", this corresponds to a linear speed of 400 cm/min.
Both pin and disc were solvent cleaned to arrive at a reproducible,
lubricant-free state. This condition is an extreme "worst case" in view
of the general practice of providing at least a monolayer of lubricant
in operating devices.

Results of the friction and wear testing are listed in
Table 4-4. For reference, the table includes test results for an Al_2O_3
surface, since this is a commonly used gas bearing material, as well as
the results for untreated beryllium. Samples 40-II and 40-III were not
received in time to be included here.

The friction coefficients given are straightforward in their
interpretation, except for the samples where material accumulated on the
wear track, a condition which is designated as "pick-up." This material
was determined to be iron or iron oxide, presumably from the steel
pin. It is therefore not surprising to see coefficients of friction for
those cases rising to values of 0.8 - 0.9 as they would in a test of
steel-on-steel.

Table 4-4. Pin-on-disc wear testing: 52-100 steel pin, 50g load.

DISC	DATE TESTED	COEFFICIENTS OF FRICTION ELAPSED TIME @ 400 CM./MIN.					EROSION 10 MIN	REMARKS
		0.1 MIN	1.0 MIN	2.0 MIN	5.0 MIN	10 MIN		
Al_2O_3	12/6/79	0.30_3	0.614			0.820	$0.13\mu^3$	AVERAGES OF SEVERAL, SOME EROSION
UNIMPLANTED I-400 Be	3/80	0.071	0.124	0.170	0.28	0.30	$1.1\mu^3$	SEVERE EROSION
60-I	12/6/79 12/12/79 4/15/80	0.20 0.11 0.15	0.23 0.20 0.27			0.43 0.76	~0	NO EROSION NO PICK-UP
60-II	4/3/80	0.178	0.29	0.75	0.89	0.90	~0	NO EROSION MUCH PICK-UP
40-I	12/6/79 12/12/79 4/15/80	0.14 0.14 0.11	0.17 0.17 0.14			0.23 0.25	~0	NO EROSION NO PICK-UP
SPIRE Hi/Lo	4/3/80	0.60	0.78	0.82	0.81	0.81	~0	NO EROSION MUCH PICK-UP
SPIRE HIGH DOSE, Hi/Lo − Lo/Hi	6/24/80	0.15	0.39			0.72	~0	NO EROSION VERY LITTLE PICK-UP

5/80 CD19739 1 81 REV A

The "wear" aspect of the test is indicated, in relative terms, under the heading "Erosion." These values are estimates of the quantity of material lost from the surface during the test, based on a simple calculation of the volume of the resulting groove.

Figures 4-5 through 4-12 are an alternative mode of assessing the test results. They show the wear tracks at 200X, microscopically and as surface profiles. Traces rising above the level of the sample surface (where there is no corresponding groove to indicate ploughing) have been interpreted as showing the "pick-up" mentioned above.

The occurence of "pick-up" is not considered to be necessarily a negative indication of sample performance in the test. Where this did occur, removal of the accumulated iron deposit from the sample with nitric acid revealed the surface to be burnished rather than damaged; see for example Figures 4-10 and 4-11. Presumably, lubrication of any sort would have reduced or eliminated the material transfer onto the implanted surface.

It may be seen by inspection of Table 4-4 and the accompanying figures that any and all implanted surfaces performed much better than the unimplanted beryllium from the aspect of erosion or wear. While this result may have been expected, there are two things which are remarkable. One of these is the better wear performance for implanted beryllium than the aluminum oxide surface, even where the coefficient of friction was approximately the same high value. The second surprising observation is the wear resistance of the SPIRE Hi/Lo implant. Although the second half of the Hi/Lo - Lo/Hi pair showed a somewhat lower friction coefficient and considerably less material transfer, the shallow 40 atomic percent implant alone appears to have been very effective in imparting wear resistance to beryllium.
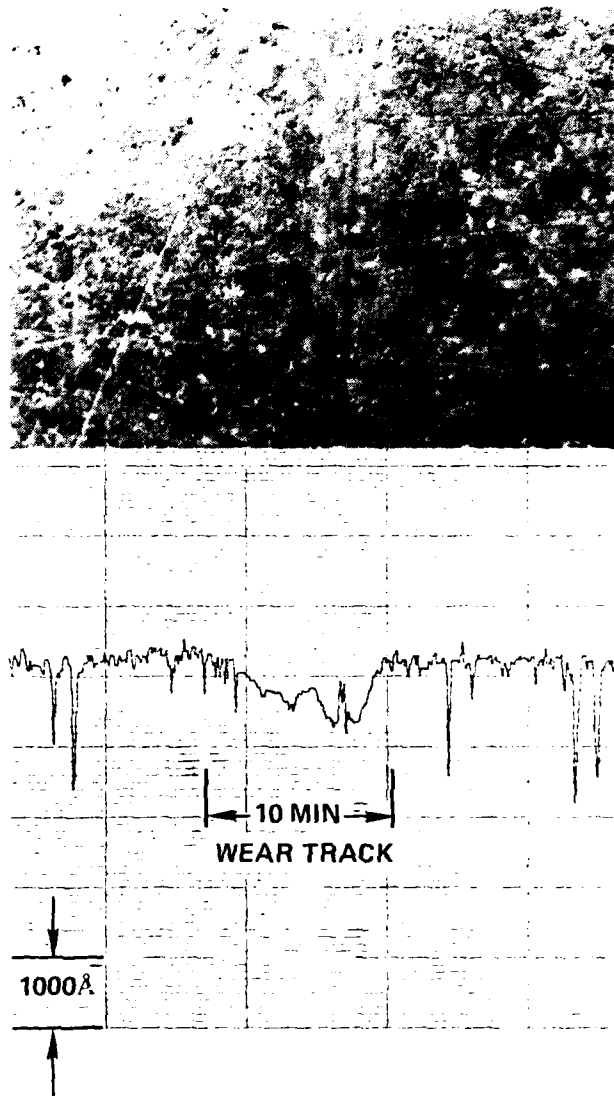
4/80 CD19500 REV A 2/81

Figure 4-5. Surface appearance and profile, Al_2O_3 after
10 minute wear test.

53

5000Å
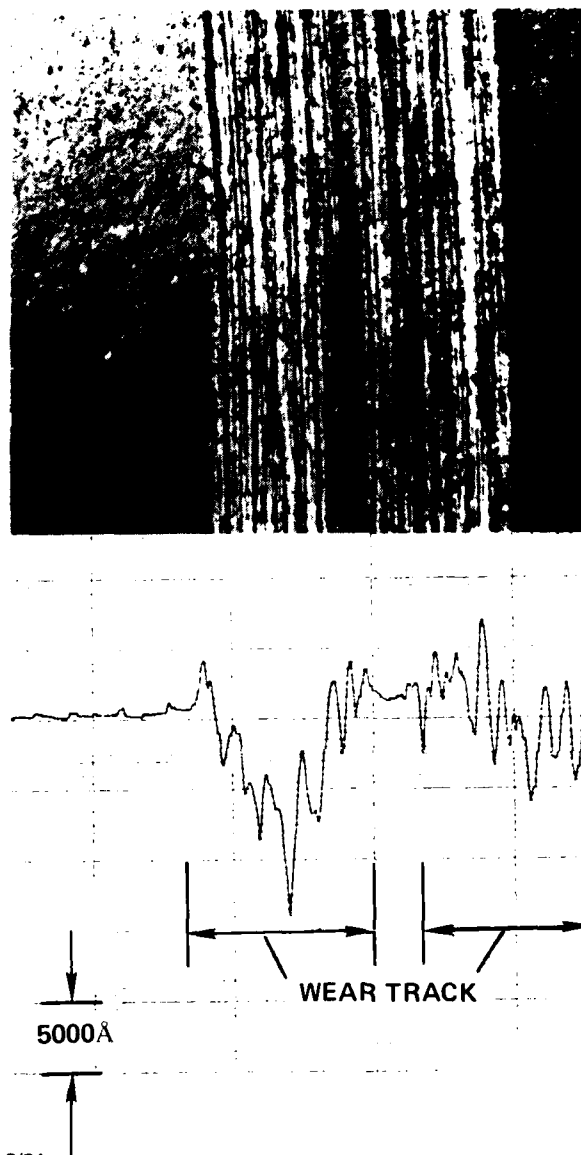
Figure 4-6.   Surface appearance and profile, unimplanted Be,
              10 minute wear test.
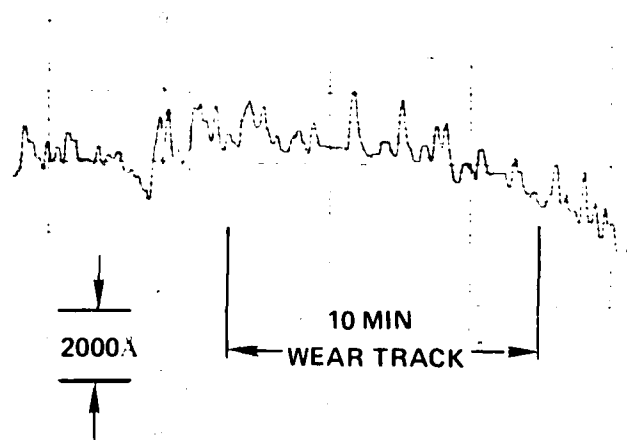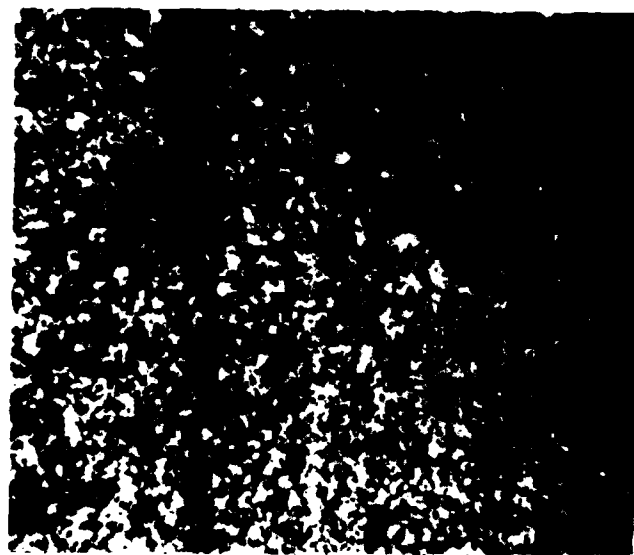
4/80 CD19502 REV A 2/81

Figure 4-7. Surface appearance and profile, 60 a/o--I after
wear testing.
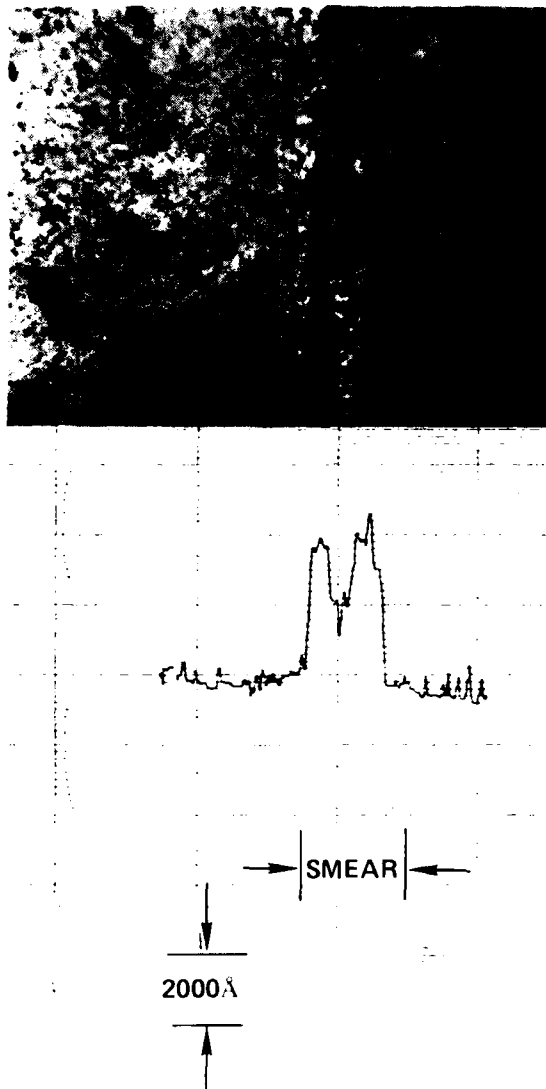
Figure 4-8.   Surface appearance and profile, 60 a/o--II
             after wear testing.

WEAR TESTING
TRACK

2000Å

Figure 4-9. Surface appearance and profile, 40 a/o after
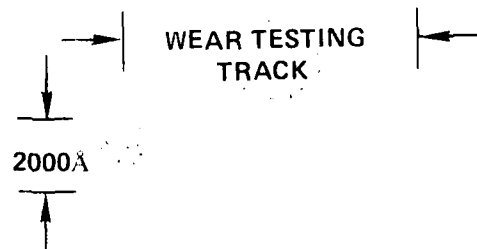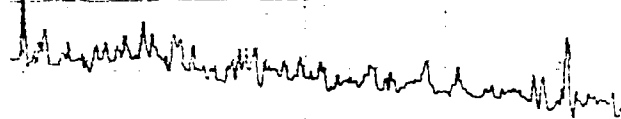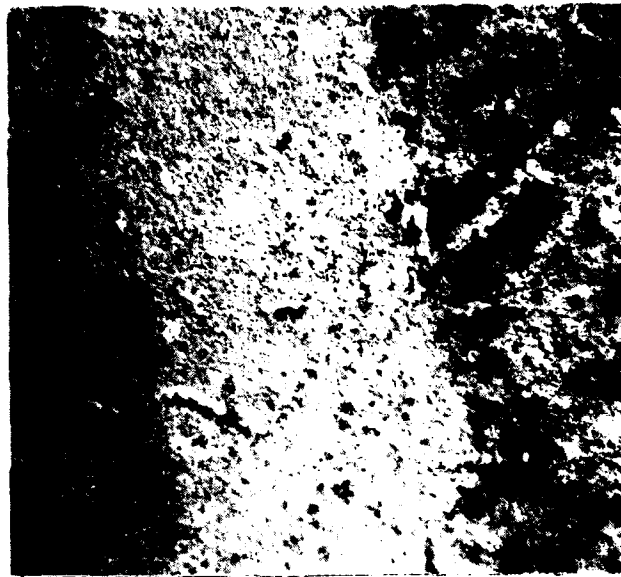   wear testing.
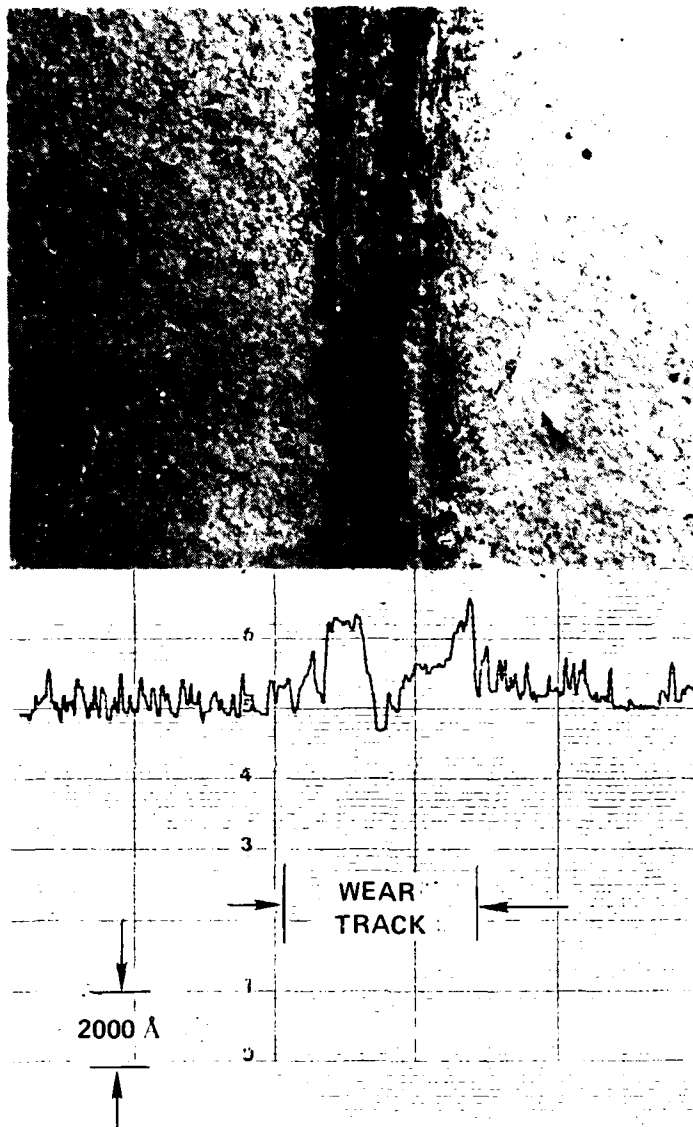
4/80 CD19505 REV A 2/81

Figure 4-10. Surface appearance and profile, SPIRE
Hi/Lo after wear testing.

WEAR TRACK

2000Å
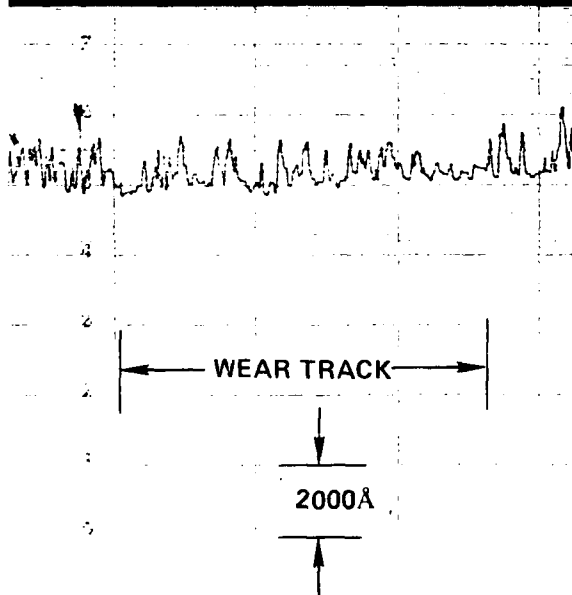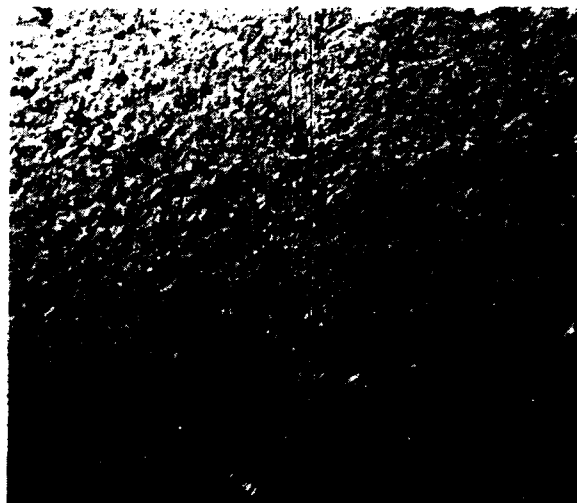
Figure 4-11. Surface appearance and profile, SPIRE Hi/Lo
after wear testing and nitric acid etch.

59
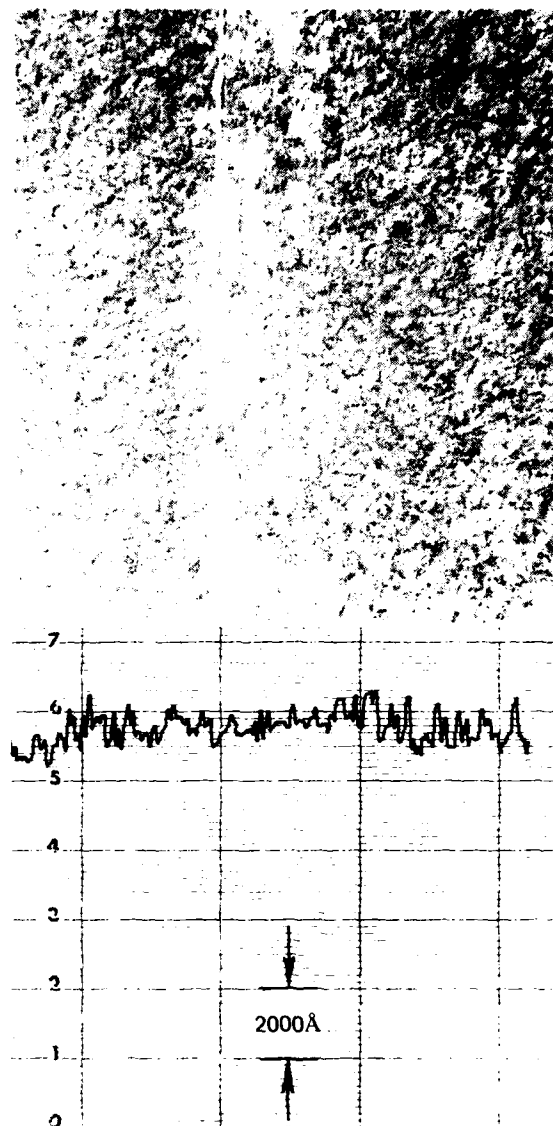
Figure 4-12.   Surface appearance and profile,
SPIRE Hi/Lo-Lo/Hi after wear testing.

60

The overall best performance in this set was displayed by the uniform implant specimen 40-I. Not only did this disc show no wear erosion but it exhibited a relatively low coefficient of friction and little or no "pick-up" from the 52-100 steel pin. For this reason, when limited implanter availability forced a narrowing of the range of concentrations to be prepared and tested in the current, graded concentration, phase of the program, it was obvious that the 40 atomic percent concentration should be the one selected for ongoing study.

4.5.6   Electron Diffraction

Originally, as noted above, the intention had been to look for beryllium boride compounds in the implanted layers by means of transmission electron microscopy and diffraction. Problems in preparing samples of the surface layers prevented this mode of study and reflection electron diffraction was tried instead.

The first candidate for observation by this technique was sample 40-I which had performed so well in friction and wear testing. (It was possibly more than coincidental that this surface had shown the highest Knoop hardness reading of those tested.)

Figure 4-13 shows the result, or rather the lack of a result. The absence of any diffraction pattern from the surface can be interpreted as showing that 1) the surface is amorphous (which is not to be expected for metals) as a consequence of implantation or 2) the metallic surface and/or beryllium boride compounds are covered over with a thin oxide film which, (especially with boron present) might be glassy and amorphous or 3) both of the above.
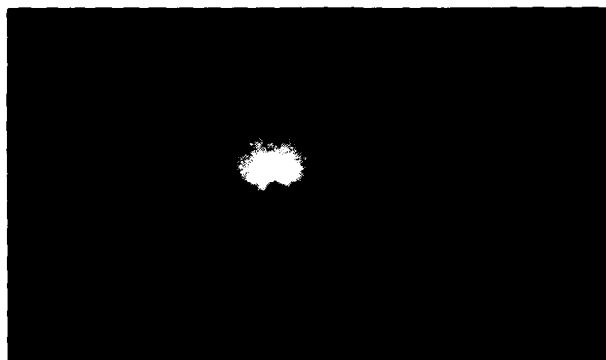
1/81 CD22548

Figure 4-13.   Reflection electron diffraction,
              40 atomic percent boron implanted in
              I-400 Be (uniform layer).

        In order to validate the method and the equipment used, it was
decided to test a known sample, i.e., the beryllium starting material.
The first attempt at diffracting an unimplanted beryllium disc gave a
result which seemed nearly as amorphous as 40-I. However, exposing the
I-400 Be sample to a standard stress-relieving heat treatment
(1450°F/1 hour, furnace cool) permitted the observation of a well-
defined beryllium diffraction pattern, together with an indication of
BeO (which is to be expected for this high-oxygen-content grade of
beryllium). See Figure 4-14. This finding tended to verify that if a
compound with a definite structure were present on a sample surface,
reflection electron diffraction should show it. It also appeared to
confirm the need for a stress-relieving heat treatment as part of the
sample preparation step.

62

As polished
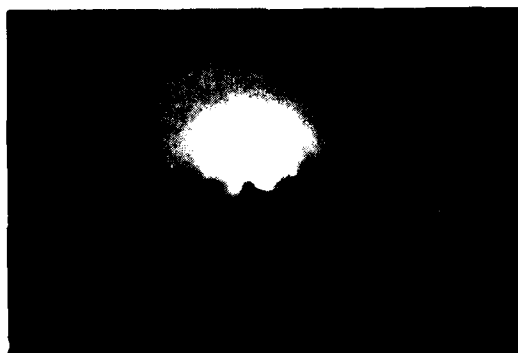
After heat treatment

1/81 CD22549

Figure 4-14. Reflection electron diffraction, unimplanted
              I-400 beryllium.

With regard to sample 40-I, the possibility still remains that a native oxide film could be interfering with the observation of existing compounds (and/or beryllium metal) although the color of the sample surface is nearly the same as the starting material. Rigorous treatments to strip off any existing oxide are being deferred until this unique sample can be studied as thoroughly as it can be by nondestructive techniques, or until it can be duplicated.

Rutherford back-scattering is one of the nondestructive techniques which were proposed for use in studying the distribution of boron within the implanted layers, but here again the limited availability of the required equipment is a problem. Although the Van de Graff generators at NRL have been used for this work in the past, there is difficulty with scheduling.

A convenient alternative is Auger analysis, which, in combination with a small area sputtering probe, can be used for concentration profiling with very limited damage to the samples. This capability has recently become available for our program and will be applied to the study of samples, particularly 40-I, during the next fiscal year.

4.6   Summary of Results

During the period of this report, testing has proceeded on previously prepared boron-implanted beryllium specimens and additional implantations have been carried out at NRL and at SPIRE Corporation. Unforeseen difficulties in polishing substrates for implantation at these locations have been overcome and this extra preparatory effort should produce more reliable results during subsequent testing.

It has been demonstrated that deterioration of the surface finish and accumulation of a surface oxide film are not necessarily associated with ion implantation processing but are avoided where there is effective temperature control and a good vacuum environment.

Variations in temperature control, and in the consequent substrate temperature rise, are believed to be the major factor in the wide divergences seen in finish retention and in the degree of hardening attained during implants which were nominally identical. The uncertainties associated with hardness measurement in general on such thin layers has been noted, but the testing is still believed to be worthwhile provided the results are seen as relative numbers and are not thought of as absolute values.

Friction and wear testing has shown that very significant improvements are imparted to beryllium by boron implantation, even when it consists of only a single shallow dose. Increased wear resistance was found to be relatively independent of microhardness readings, probably because the latter do not accurately indicate the true hardness values of the very thin layers involved.

Preliminary tests of the concept of the graded layer, achieved by high energy implantation through either a sputter-deposited boron film or a shallow heavily implanted layer, have been encouraging with regard to both wear resistance and surface hardening.

Proof, by electron diffraction, of the existence of beryllium boride compounds within the implanted layers has yet to be demonstrated. The indication that the implanted layer becomes amorphous has yet to be made credible by confirmation.

4.7   Direction of Further Work

While only very limited numbers of graded layer specimens have
been prepared to date, there are presently available sufficient numbers
of stress-relieved polished substrates to allow multiple sample
preparations. This will produce better verification of findings through
repeated testing, and the results obtained will be of higher validity
because of the greater care (stress relief, better flatness and finish)
given to the preparation of the starting material.

Multiple samples of graded layers of both types, the all-
implanted type and the "hybrid" pre-coated type, will be prepared. At
the same time, several repeats of uniform concentration layers will be
prepared, allowing correlation with earlier implants carried out under
somewhat different conditions.

Substrates, when implanted, will be given more positive heat
sinking for better temperature control. In addition to better retention
of flatness, finish, and freedom from oxide films, this should allow
evaluation of the effect of temperature separately from the effect of
boron dose when the substrates are tested before and after heat treatment.

Future friction and wear testing will include substitution of an
aluminum oxide or tungsten carbide tip for the 52-100 steel pin. Test
fixturing has been modified to accept 0.125" diameter balls of these materials
as a stylus, but the smaller radius of curvature gives a much higher stress.
The loading must therefore be recalculated to make the conditions comparable
to previous test runs, as some preliminary trials have indicated.

A newly available improved Auger profiling procedure will be
applied to the search for beryllium boride compounds in the implanted
layers. Using this in conjunction with reflection electron diffraction
will assure freedom from interfering native oxide films; it will also
indicate promising levels, within the layers, to be studied by diffraction
methods.

Finally, arrangements are being made to implant grooved beryllium thrust plates of an existing type of device with the objective of evaluating boron implanted beryllium as a gas bearing. The implantation and heat treatment schedules will be those which promise the best performance, based on results from the current test specimens.

SECTION 5.

COMPOSITE MATERIAL

As an alternative approach to the fabrication of a hard, wear-resistant gas bearing surface, the inclusion of an investigation aimed at the development of a composite material was proposed and included in the Office of Naval Research (ONR) sponsored research in October 1979. The composite was proposed to consist of a dispersion of ceramic particles in a beryllium metal matrix and was to be formed by hot isostatic pressing of cold isostatically pressed compacts of beryllium and ceramic powders. The physical properties of such a material were, therefore, expected to lie between that of ceramic and beryllium. The properties of such a material should be much more compatible to the rest of the structural gyro members than those of a solid ceramic. The entire wear and friction process in this material will be confined to the ceramic particles standing out in relief at the surface of the composite. Using near net-shape technology, it will also be ultimately possible to drastically reduce the machining costs that were encountered earlier when bearing fabrication was attempted from solid pieces of ceramic.

5.1   Material Selection Criterion

A review of the literature available in the areas of friction and wear shows a considerable lack of understanding of these phenomena in the ceramic materials [18] . This has resulted partly from the complexity of the problem and partly because the bulk of research has been confined to investigations on metallic systems. Little effort has been directed, so far, at understanding sliding wear mechanisms in the ceramic nonmetals.

The value of the coefficient of friction is found to be low for the ceramic materials. Low friction value is of interest because it permits operation of the gas bearing at low starting torque levels. Besides this, the designer is primarily concerned with the wear-resisting ability of the surface.

No single, reliable, physical parameter was known to exist to help us select the most suited material. The only guiding value appeared to be the microhardness in kg/mm^2. This was unfortunate since hardness per se does not appear to completely explain wear behavior, even though it is found to be an important parameter. A high value of hardness, however, indicated strong interatomic bonds and, in lieu of a better criterion, had to suffice as the rationale for selection of the ceramic needed to satisfy the surface (friction and wear) requirements of the gas bearing. Hard materials are also known to be resistant to wear from impact and erosion processes. Evidence obtained on metal-ceramic composites has also indicated that composites which have high average values of microhardness are also more resistant to abrasive wear [20]. (Average microhardness of a composite is defined as the total of the contributions of the microhardness values of the metal and ceramic calculated in proportion to their respective volume fractions in the composite.) It was necessary, therefore, to select a hard ceramic for fabrication of the beryllium-ceramic composite from a wear and friction point of view.

Other considerations examined were the chemical and thermal expansion compatibility of the chosen ceramic with beryllium and the machinability of the fabricated composite. Chemical compatibility (as indicated by the values of the free energies of formation of the several compounds) is important in these metal-ceramic systems because even though it is desirable that the metal matrix wet the ceramic, one does not want the metal to chemically reduce the ceramic at the temperature used for densification. Examples of unstable systems are the UO_2-Al and the ZrO_2- (V-Ni alloy) metal-ceramic systems. An example of a stable

system, on the other hand, is the UO_2-Cu system. Effects related to thermal expansion compatibility are, likewise, equally important. In cases where the ceramic phase has a higher expansion coefficient than the metallic phase (as in the UO_2-Mo system), the ceramic particles will tend to separate (upon cooling from the densification temperature) from the metal matrix. Cracks are generally observed at the phase boundary in such instances. This situation is more pronounced for ceramic particles that are spherically shaped as opposed to irregularly shaped particles where mechanical interlocking between the phases gives rise to stronger adhesion of the particle to the matrix. If, on the other hand, the metallic phase has a higher expansion coefficient than the ceramic phase, the ceramic particles will be subjected to a compressive stress. A mild compressive state may actually promote good wear behavior of the ceramic since ceramics are known to perform better under a compressive loading. Too high a stress level may, however, have quite the opposite effect because of the unequal stress distribution that would result in the ceramic particle when it is exposed at the surface. Finally, machinability of the composite which was not known when the ceramics were selected is expected to be examined at a later stage of this program (primarily from a cost standpoint). For similar performance it would certainly be desirable to use a composite that is easier to machine because this will result in reduced fabrication costs of the gas bearing. It is possible to substantially reduce machining costs by developing a near-net shape fabrication technology.

Because of these several theoretical considerations, three different types of ceramic powders were selected to separately form the composite with beryllium. The ceramics selected were aluminum oxide (Al_2O_3), titanium carbide (TiC), and titanium diboride (TiB$_2$).

5.2   Previous Work

Be-TiB$_2$ composite material fabricated earlier (during initial experiments at CSDL) using the hot isostatic pressing technique had demonstrated that the fabrication sequence in itself needed a certain

amount of development effort [21]. The micrograph contained in Figure 5-1 shows the poor densification obtained in a sample that was isostatically densified at 900°C temperature and 15 klb/in.^{2} gas pressure for 2 hours. Large pockets containing loose TiB$_2$ powder (which was the chosen ceramic) were observed with the unaided eye. The observed defects were attributed to poor blending (which was done by gently tumbling the powders in a V-shaped conventional laboratory blender), insufficient outgassing of the powders (which was performed at 400°C prior to sealing the powder compacts in metal cans before densification) and a possibly lower than optimum densification temperature (900°C in this experiment). This problem, was therefore, corrected to a considerable extent by resorting to higher energy powder blending (in a ball mill), outgassing of the powders at 600°C prior to container encapsulation, and using a slightly higher densification temperature (950°C). The improvements in structural uniformity and material integrity that resulted from these steps are evident in the photograph shown in Figure 5-1(B). (The variation in observed ceramic grain size is attributed to the selection of the starting powder, designated as -325 mesh, or less than 45 microns, therefore indicating a wide range of particle sizes.

5.3   Present Work

5.3.1   HIP Fabrication of Samples

Beryllium powder, designated as -325 mesh, was blended with selected samples of the different ceramics (Al$_2$O$_3$, TiC, and TiB$_2$) using the high energy blending procedure discussed above. Ceramic powders were obtained in different sizes of -325 mesh (less than 45 μm) and 1-2 μm from a commercial source. These were separately mixed with the beryllium to yield powder blends containing 40 and 55 volume percent of ceramic. The variations that were therefore attempted pertained to type, percent volume, and particle size of the ceramic. The blended

(A)

⊣ ⊢— 100 μm

(B)
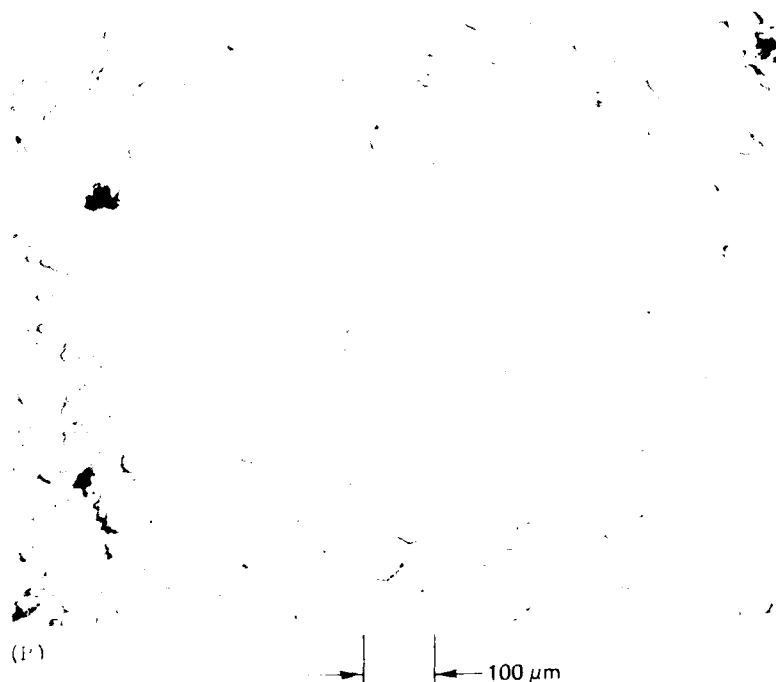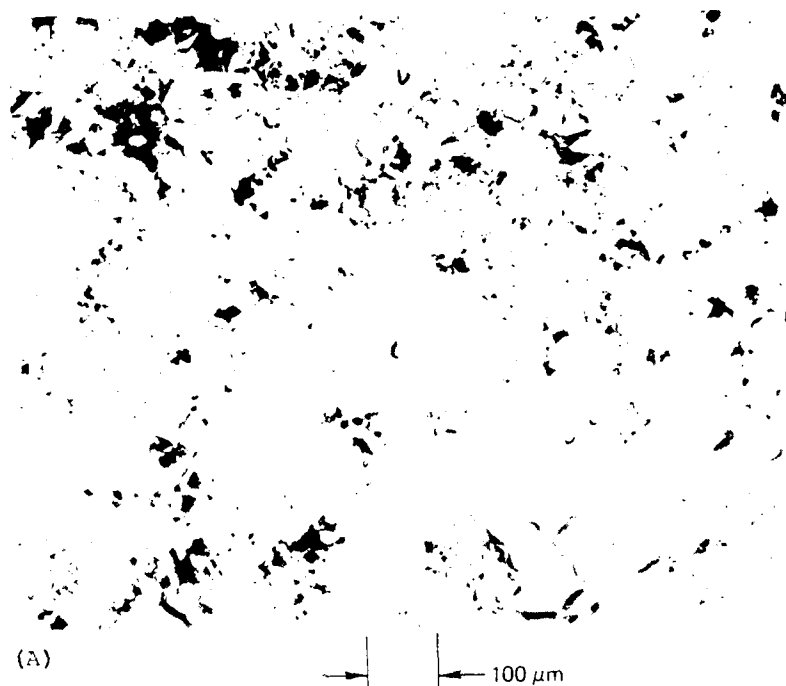
1/81 CD22550

Figure 5-1. TiB₂ dispersion in Be matrix. (A) Poor densification and dispersion; (B) improved densification and dispersion. As polished.

73

powders were then placed inside rubber boots and cold isostatically-pressed at a pressure of roughly 55 klb/in^2. Care was exercised not to subject the rubber boot to vibratory motion during the initial filling to minimize sedimentation effects that could result from density differences between the two powders (beryllium and ceramic). This initial filling was accomplished through a gentle tamping action on the powder using an extended piston-like tool. All of the beryllium handling was performed in a hood designed specifically for such purposes, while adhering to strict safety procedures.

The green compacts, obtained after cold isostatic pressing, were placed in low carbon steel containers and the vessels sealed with an exit tube attached to one end. The enclosed samples were outgassed at a temperature of 600°C to a predetermined level of vacuum. At this point, the exit tube was also sealed through a hot pinching process and the samples were ready for hot isostatic pressing (HIPing). Based on earlier work, the samples were HIPed at a temperature of 975°C and an inert gas pressure of close to 15 klb/in.^{2} in a high temperature autoclave at an outside vendor's facility. From the way the containers had collapsed during HIPing it was tentatively concluded that all samples, except two, had been successfully pressed.

To remove the HIPed material from inside the low carbon steel containers, it was determined that an acid dissolution tecnnique that preferentially dissolved the steel cans (and had little or no effect on the beryllium) would be more desirable than conventional machining procedures. Experiments were successfully performed to this end using a warm 50 percent solution of nitric acid (HNO_3). The container material was observed to dissolve quite rapidly and the reaction visibly stopped at the composite surface. The cost savings, achieved by following the acid dissolution procedure that was developed, are expected to be even more substantial when attempts are eventually made to fabricate intricate pieces of actual gas bearing hardware to near-net shape using this material.

Disc-shaped samples, 0.75-inch in diameter and about 0.3 inch long, were next attempted from each of the composite materials for further evaluation. In agreement with earlier experience at CSDL, it was found that conventional machining on a lathe was both expensive and time consuming. Tungsten carbide tools were found to wear away at a very rapid rate with very little machining effect on the actual composite. To reduce these costs (of sample preparation), the electrical discharge machining (EDM) process was investigated. Experiments showed that these materials could indeed by EDMed but only very slowly (at a rate somewhat similar to conventional machining). EDM was nevertheless chosen as the preferred technique because of the much lower labor and material costs incurred using this procedure. All of this underlined the eventual need for developing a near-net shape fabrication technology for actual hardware applications which could be coupled with a grinding and lapping procedure to produce parts at reasonably low cost.

A format which included a four-digit number followed by a letter was selected for sample identification. The first two digits indicated volume percent, the next two the particle size in microns, and the fifth position was occupied with a letter indicative of the ceramic. The letters O, C, and B correspond to the ceramics Al_2O_3, TiC, and TiB_2 respectively. For instance, sample 4045 B stands for a composite containing 40 percent TiB_2 in a matrix of beryllium with a ceramic particle size designated as -325 mesh (or less than 45 microns). After one disc was obtained from each of these materials, a density measurement was obtained on each sample using the wet displacement technique. The values measured and how they compared with theoretical expections are shown in Table 5-1. Table 5-1 also shows that of the 10 samples that were believed to be successfully HIPed from visual examination of the HIP containers, only seven were deemed acceptable for further experimentation on the basis of density considerations. An additional disc-shaped sample, similar to the ones procured earlier, was then EDMed from each of the seven acceptably densified composite materials.

Table 5-1. Density measurements on HIPed samples.

SAMPLE NUMBER	DENSITY (g/cm^3)	PERCENT THEORETICAL	ACCEPTABLE
4001 B	2.68	92	yes .
4001 O	2.59	96	yes
4001 C	2.62	85	no
5501 B	3.06	93	yes
5501 O	2.85	94	yes
5501 C	2.89	85	no
4045 B	2.91	100	yes
4045 C	2.74	89	yes?
5545 O	3.05	100	yes
5545 C	3.05	86	no

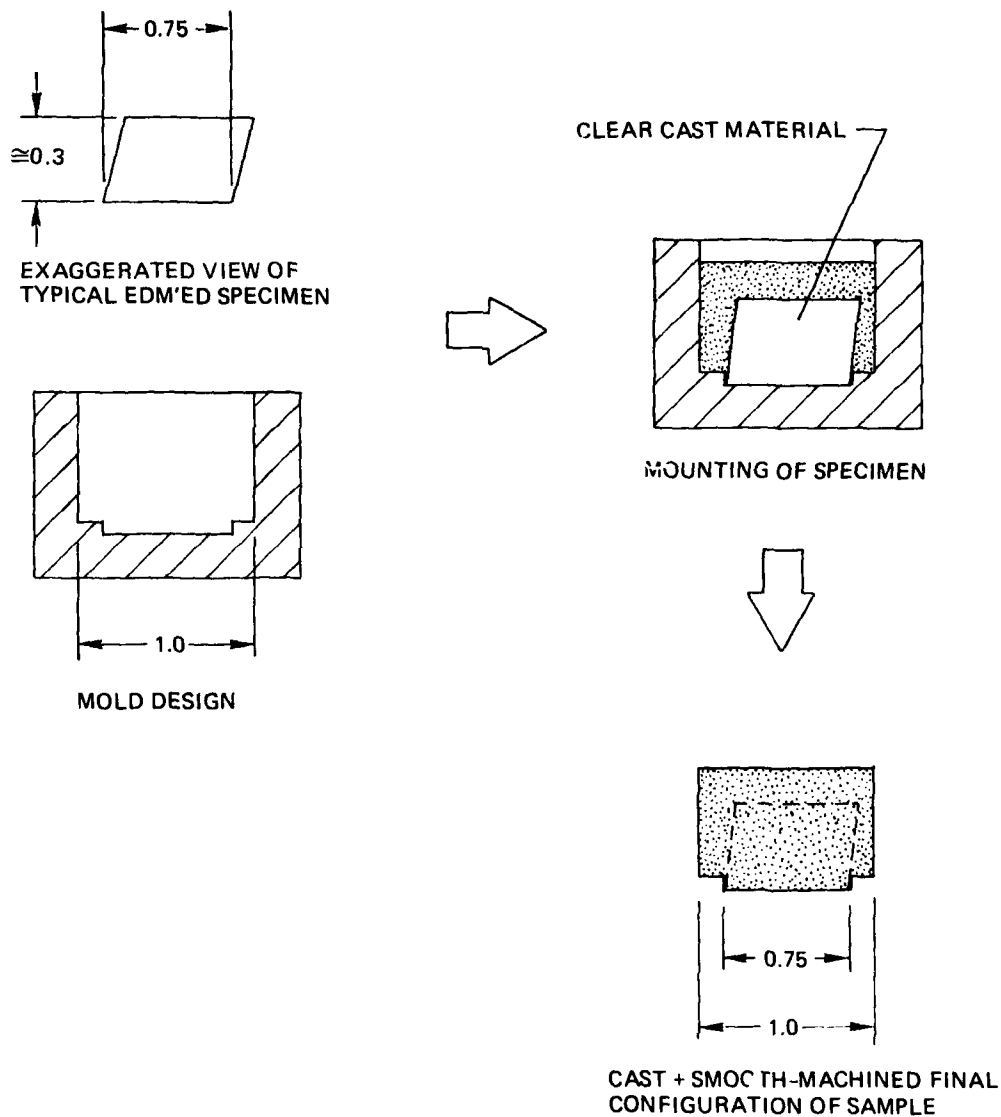Density values used for calculating theoretically attainable density in composite were:

Be   - 1.85 g/cm^3
TiB_2 - 4.50 g/cm^3
Al_2O_3 - 3.98 g/cm^3
TiC   - 4.92 g/cm^3

Even though EDM permitted the removal of samples with disc geometry from the densified materials, it was observed that the cylindrical surface in many of the samples was not oriented exactly perpendicular to the flat ends. This posed a problem in that these samples were designed to be tested for wear and friction in a disc-on-disc geometry after appropriate preparation of the sample surface. For tilted specimens, application of a uniform load over the whole surface during testing (as well as during controlled lapping operations on a Crane Lapmaster) and alignment of mating discs could conceivably have posed a problem. Therefore, a rubber mold was designed so that the specimens could be mounted in a resin containing clear-cast material with about 1/16 inch of the sample sticking out of the mount and its external surface concentric with the mounting material. The samples were cast in this form with the exposed surface of the mount material smooth-machined to a diameter of 1.0 inch. The overall thickness of the sample (and the mount) was maintained at about 1/2 inch. A schematic sketch of the problem and its solution are shown in Figure 5-2. At this point the samples were considered ready for lapping operations.

5.3.2   Study of Lapping Effects

Preparation of the sample for wear testing using a disc-on-disc geometry requires intimate contact between mating surfaces. For this reason, the surfaces should be quite flat. This can be accomplished by following controlled lapping procedures.

Lapping was performed after placing the specimens on a Crane Lapmaster. The lap was charged with progressively finer sizes of Al_2O_3 containing compounds, the disc samples placed on the lap, a given dead load applied to the samples, and the machine turned on. (It was recognized that diamond containing lapping compounds were actually more desirable, but use of the diamond materials would have required the availability of several machines - one for each particle size. Since only one such lap was available, it was decided to pursue these experiments, instead, with Al_2O_3 containing compounds which could be

77

0.75

≅0.3

EXAGGERATED VIEW OF
TYPICAL EDM'ED SPECIMEN

CLEAR CAST MATERIAL

MOUNTING OF SPECIMEN

1.0

MOLD DESIGN

0.75

1.0

CAST + SMOOTH-MACHINED FINAL
CONFIGURATION OF SAMPLE

1/81 CD22551

Figure 5-2. Schematic sketch of sample mounting procedure.

78

effectively removed by cleaning from the lap before applying a fresh
charge of polishing compound. At a later stage of this program,
however, it is intended to examine lapping effects in these materials
through hand-held procedures using diamond compounds on a mehanite
lap. Such laps are used at CSDL during lapping of actual gas-bearing
hardware.)

Detailed observations on effects arising from the lapping of
these materials, with Al_2O_3, were made on discs made from a 3545 B
sample that was produced earlier. These studies showed that use of
coarse (500 grit size) particle Al_2O_3 resulted in the ceramic particles
standing out considerably in relief above the beryllium surface.
Scanning Electron Microscopy (SEM) observations showed that the surface
of the recessed beryllium after polishing with coarse particles was also
quite rough after this polishing procedure (see Figure 5-3). When this
sample was subsequently polished with the finer Al_2O_3 pastes (the finest
contained a 2 to 3 μm Al_2O_3 particle size) micromachining of the TiB_2
particles was observed. This is believed to have continued until the
height of the ceramic particles was reduced to that close to beryllium,
beyond which point both the beryllium and the micromachined ceramic
particles were subjected to a simultaneous polishing action. It is
suspected that the step height between that of the ceramic and the
surrounding beryllium would be a direct function of the coarseness of
the polishing particles principally because the ceramic wears away at a
much slower rate than does the beryllium. The observations relating to
the micromachining effects discussed above are shown in Figure 5-4.
Figure 5-4 also contains a SEM photograph obtained on this same sample
after selectively dissolving the beryllium (relative to the ceramic) for
about 2 to 5 seconds using a KBI etch *. This etchant was developed

---

* KBI etch consists of 500 milliliters H_2SO_4 +
500 milliliters Phosphonic Acid + 750 grams Chronic Acid +
3 liters water (use at 50°C).

(A)

|← 50 μm →|

(B)
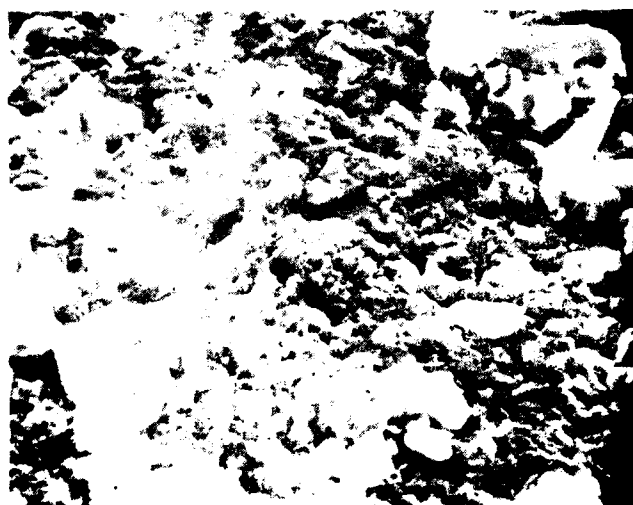
|← 20 μm →|

Figure 5-3. As-polished 3545 B surface using coarse Al_2O_3 paste. Different magnifications.

(A)

$\longmapsto \longmapsto$ - 50 μm


(B)

$\longmapsto \longmapsto$ 50 μm
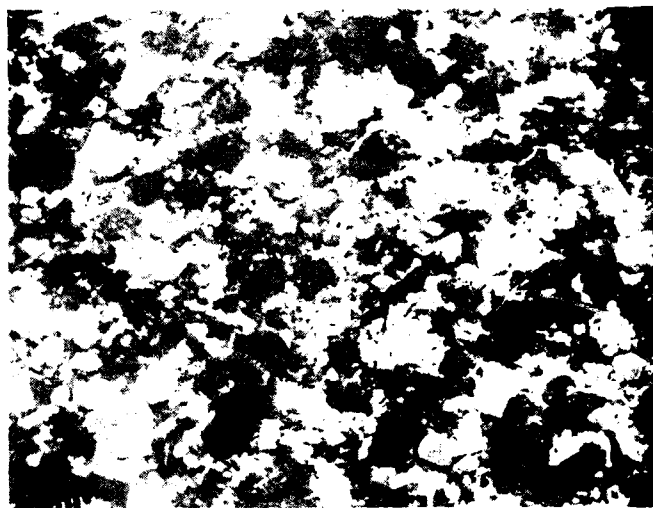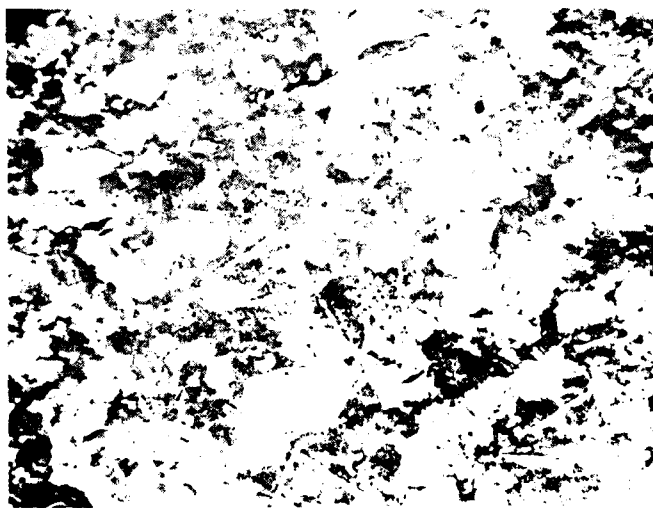
1/81 CD22553

Figure 5-4. Micromachining effects on ceramic particles. Sample 3545 B. (A) As-polished; (B) after 2 seconds KBI etch.
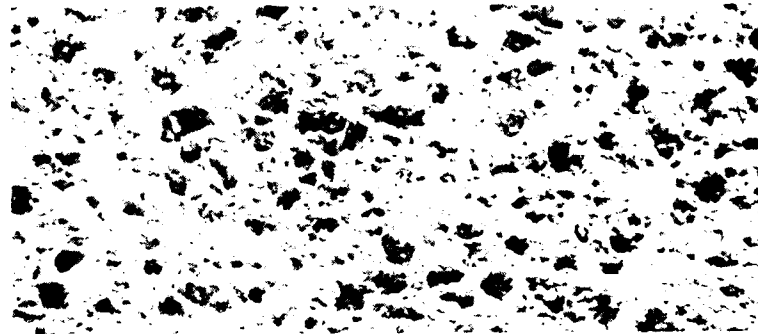
-1

earlier by the Kawecki Berylco Company. Figure 5-4 shows that the step height between the beryllium and the ceramic can possibly be adjusted by varying the time of etching. Some pitting of the beryllium matrix was, however, seen as a result of the chemical reaction of the etchant with the beryllium.

Sample discs, two from each HIPed composite (each disc mounted with its flat surface concentrically located in a resin containing clear cast material), were subsequently polished using the above procedures. The microstructures that were generated in some of these samples, as revealed by SEM, are shown in Figure 5-5. The SEM photographs were obtained on the as-polished surfaces. An electrical conducting path from the sample to the specimen stage in the SEM was provided by drilling an 1/8-inch hole in the rear side of the sample (through the clear-cast material) and using silver paste to provide the conducting path.

One of the more noteworthy observations made during this study is shown in Figures 5-6 and 5-7, and is basically related to ceramic particle distribution in the composite. These SEM micrographs show that the -325 mesh ceramic particle containing composites were more desirable than were the 1 to 2 micron containing composites. Whereas the -325 mesh samples showed a reasonably uniform distribution of the particles throughout the beryllium matrix, the 1 to 2 micron samples showed that the ceramic particles were mainly segregated at the grain boundaries of the beryllium. Also, the 1 to 2 micron ceramic particles were not completely surrounded by the beryllium as compared to the -325 mesh particles which showed an intimate physical contact between the ceramic and the beryllium (all around the ceramic particle). It is possible that these fine ceramic particles would also have a greater tendency to become dislodged from their positions during surface rubbing operations. Micromachining effects of the ceramic particles were not observed in the 1 to 2 micron samples, possibly because of their very small ceramic particle size, and maybe even because of a lowered tendency of the particles to remain bonded to the matrix.

82
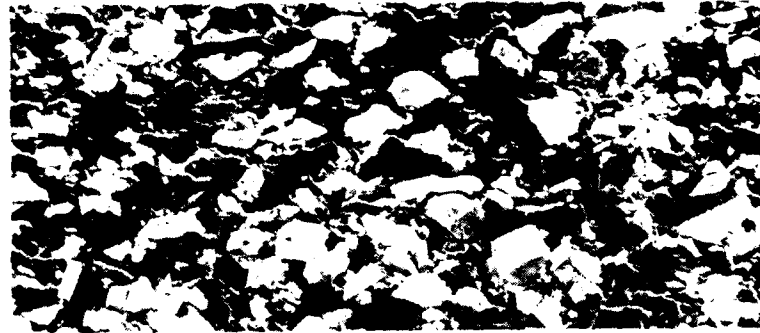
(A)   ⊢ ⊢— 50 μm

(B)   ⊢ ⊢— 50 μm

(C)   ⊢ ⊢— 10 μm

1/81 CO22554
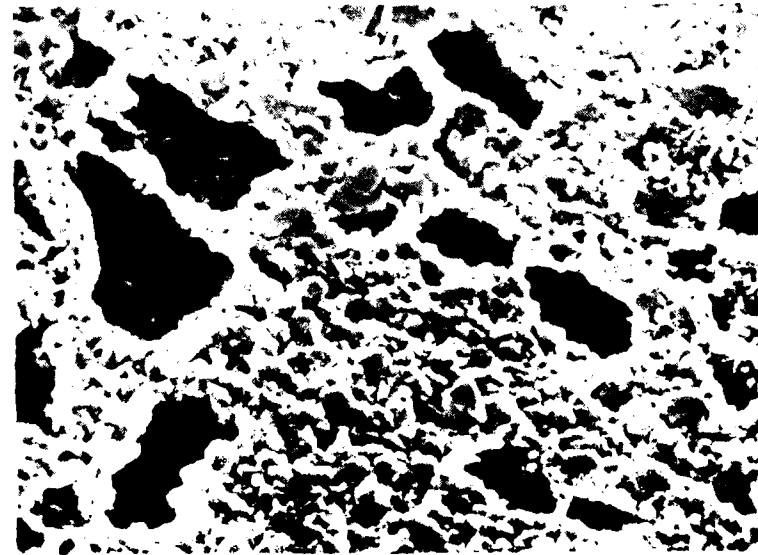
Figure 5-5.   As polished SEM photographs of selected samples.
(A) 3546-9; (B) 4046-3; (C) 5501-6.

(a)

◄—————► 50 μm

(b)

◄—————► 50 μm

Figure ... SEM microstructure ... observed ...
... observed ...

(A)

|← →| 10 μm

(B)

|← →| 5 μm
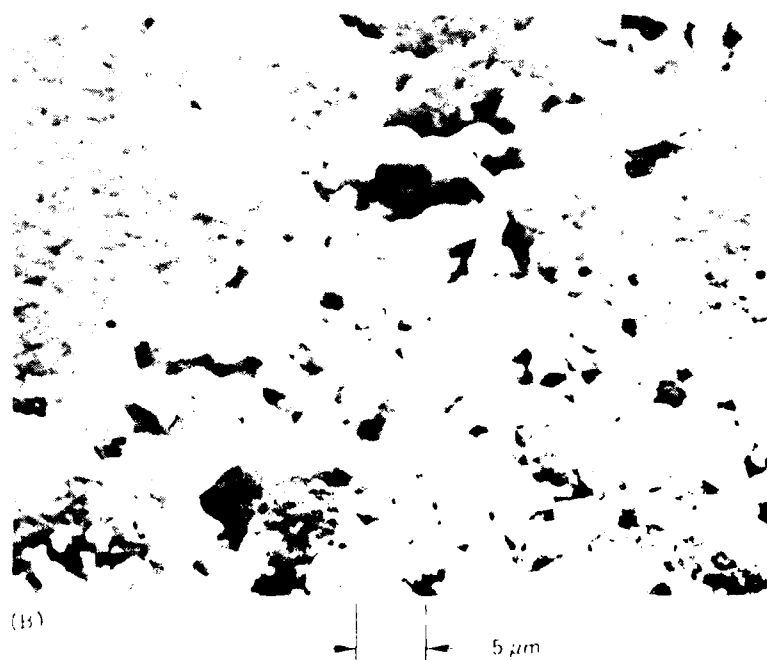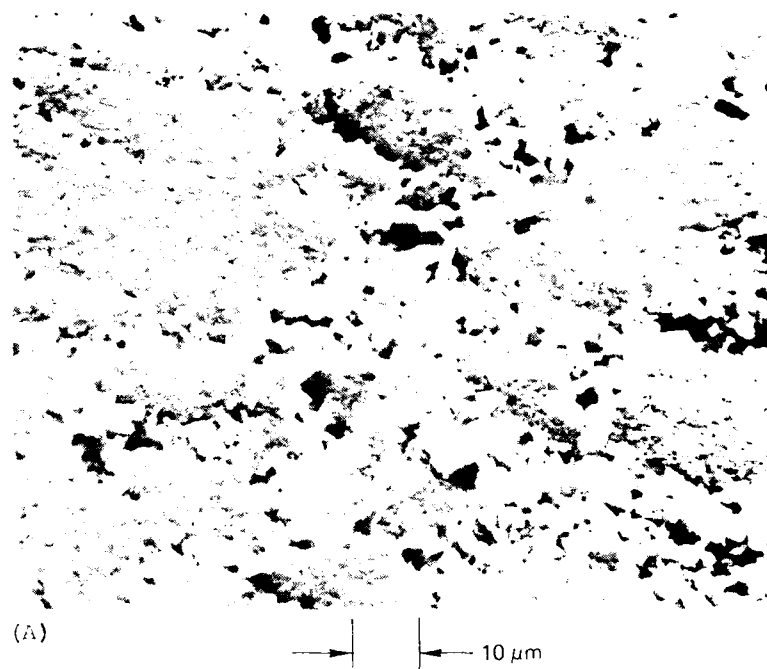
1/81 CD22556

Figure 6-7.   Higher magnification SEM photographs of 4001 B.
               Fine particles are clearly observed in grain
               boundary regions.

97

Another significant observation made during these investigations was the near-absence of micromachining of the ceramic particles in the Al_2O_3 containing 5545-0 composite. The SEM observations on the as-lapped condition of this composite showed the existence of reasonably large voids in sizes comparable to the -325 mesh Al_2O_3 particles. These voids must have clearly resulted from Al_2O_3 particle pull-out during the several lapping operations it was subjected to during disc sample preparation. This view is directly supported by the microstructure observation in Figure 5-8 (and also in Figure 5-5(A) that show that void shape is similar to particle shape, and by the density measurement which shows that the as-pressed density of this material was close to what was theoretically considered the maximum. Furthermore, any voids formed at the HIP temperatures, due to inadequate sintering, are expected to be close to spherical in shape and not possess the irregular features that were observed for this sample. It is, therefore, reasonable to assume that the observed voids are actually areas where Al_2O_3 particles were pulled-out from during polishing. This also accounts for the absence of ceramic particle machining effects, since the Al_2O_3 composite particle was more susceptible to removal from the matrix than to being abraded at the surface. All of this indicated extremely poor bonding of the Al_2O_3 particles to the beryllium matrix.

5.4   Conclusions and Future Work

Future work will be primarily concerned with microstructure optimization of TiB_2 containing Be - ceramic composite materials. This study has already significantly demonstrated that larger particle sizes of the ceramic are more desirable for mixing with -325 mesh beryllium powder to produce composites with reasonably well-defined dense microstructures. We have also found that poor bonding occurs between beryllium and the Al_2O_3 particles indicating the unsuitability of fabricating such composites with this type of ceramic. This study has

1.0

2.8 2.5

3.2 2.2

3.6

2.0

1.1

1.8

1.25 1.4 1.6

MICROCOPY RESOLUTION TEST CHART

50 μm
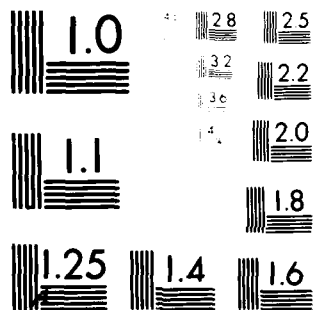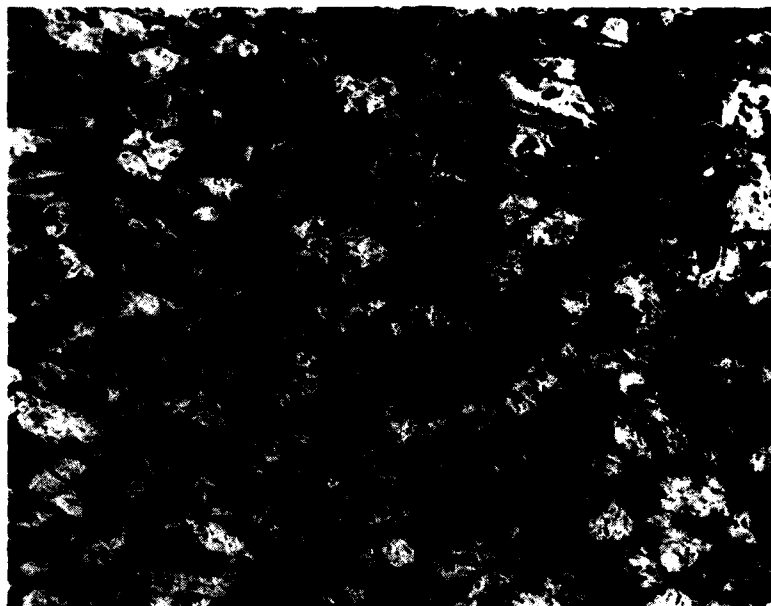
1/81 CD22557

Figure 5-8. As-polished 5545 O surface. Large voids observed
with void shape similar to that observed for the
particles. Micromachining of Al_2O_3 particles in
these samples was not observed.

87

further shown that the TiC powder used is possibly difficult to outgas, therefore, acceptable densities could not be attained. All of the above suggests that most of the future effort should be concentrated on composites containing TiB_2 as the ceramic constituent. In addition to microstructure definition of such ceramics (primarily from the point of view of good wear and friction characteristics), measurement of physical properties such as thermal expansion and thermal conductivity will also be performed. Fabrication of actual hardware pieces is additionally planned.

REFERENCES

1. Keating, W.H., <u>Compliance Coefficient Test Results for TGG</u>
    <u>No. 222X</u>, Component Development Department, Memorandum No.
    30H-76-541, The Charles Stark Draper Laboratory, Inc.,
    December 1976.

2. Kumar, K., <u>Analysis of $W_{(x)}$ C Sputter Deposits</u>, Report No.
    C-4749, The Charles Stark Draper Laboratory, Inc., October
    1976.

3. Rutherford, J.L. and W.B. Swain, <u>Alumina Bearing in Gas-</u>
    <u>Lubricated Gyros</u>, AIAA/ASME 8th Structures, Structural
    Dynamics and Materials Conference, California, NASA Report
    No. NASA-CR-88597, 29-31 March 1967.

4. <u>Advanced Inertial Technologies</u>, Vol. III, Technical Report
    AFAL-TR-73-124, The Charles Stark Draper Laboratory, Inc.,
    March 1974.

5. McEwen, J., and R. Schluntz, <u>History and Experience into</u>
    <u>Chromium Oxide (LC-4) Plasma Coating of Bearings by Union</u>
    <u>Carbide</u>, Report No. C-4699, The Charles Stark Draper
    Laboratory, Inc., July 1976.

6. Markovsky, L. Ya, Yu, D. Kondraskev, and G.V.
    Kaputovskaya, <u>The Composition and Properties of Beryllium</u>
    <u>Borides,</u> J. Gen. Chem. U.S.S.R., Vol.25, 1955, p. 1007.

REFERENCES (Continued)

7.   Tupitsyn, I.I., I.I. Lyakhavskaya, M.S. Nakhmanson, and
        A.S. Sukhik, Energy Structure of Beryllium Diboride, Sov.
        Phys. Sol. State, Vol. 16, No. 16, April 1975.

8.   Hoenig, C.L., C.F. Cline, and D.E. Sands, Investigation of
        the System Beryllium-Boron, J. Am. Ceram. Soc., Vol. 44,
        No. 8, p. 385, August 1961, p.p. 385.

9.   Laubengayer, A.W., D.T. Hurd, A.E. Newkirk and J.L. Hoard,
        Preparation and Properties of Pure Crystalline Boron, J.
        Am. Chem. Soc., Vol. 65, 1943, p.p. 1924.

10.   Croft, W.J., N.C. Tombs, and J.F. Fitzgerald, Preparation
        and Characterization of Boron Films from Diborane, Mat.
        Res. Bull., Vol. 5, 1970, p.p. 489.

11.   Kumar, K. and D. Das, Structure Modification of β -Boron
        by Plasma Spraying, Met. Trans., Vol. 11A, 1980, p. 1489.

12.   Hirvonen, J.K., J. Vac. Sci. Technol. 1 s, 1978, p. 1662.

13.   Liau, Z. L. and J.W. Mayer, J. Vac Sci Technol. 1 s 1978,
        p. 1629.

REFERENCES (Continued)

14. Kant, R.A., J.K. Hirvonen, A.R. Knudson and J.S. Wollam, Surface Hardening of Beryllium by Ion Implantation, Thin Solid Films 63, 1979 pp. 27-30.

15. Das, D., K. Kumar, E. Wettstein, J. Wollam, Materials Research for Advanced Inertial Instruments, Task 2. Gas Bearing Material Development by Surface Modification of Beryllium, Technical Report R-1330, The Charles Stark Draper Laboratory, Inc., October 1979.

16 Tsaur, B.Y., Z.L. Liau, and J.W. Mayer, Appl. Phys. Lett. 34, 1979, p. 168.

17. Hartley, N.E.W., "Tribological Effects in Ion-Implanted Metals," in Applications of Ion Beams to Materials, Institute of Physics, London, 1976, p.p. 210.

18. Rabinowicz, E., Friction and Wear of Materials, John Wiley and Sons, Inc., New York, 1965.

19. Lysaght, V.E. and A. Debellis, "Hardness Testing Handbook," Amer. Chain & Cable Co.

20. Ondracek, G., B. Leder, and C. Politis, Quantitive Metallography of Metal-Ceramic Composites, Prakt. Metallogr., 5 (2), 1968, pp. 71-84.

21. Technical Proposal for Office of Naval Research, Materials Research for Advanced Inertial Instrumentation, CSDL Proposal No. 9-821, May 1979.

BASIC DISTRIBUTION LIST

Organization	Copies	Organization	Copies
Defense Documentation Center Cameron Station Alexandria, VA 22314	12	Naval Air Propulsion Test Center Trenton, NJ 08628 ATTN: Library	1
Office of Naval Research Department of the Navy 800 N. Quincy Street Arlington, VA 22217		Naval Construction Batallion Civil Engineering Laboratory Port Hueneme, CA 93043 ATTN: Materials Division	1

ATTN: Code 471
        Code 102
        Code 470
	1
	1
	1
		Naval Electronics Laboratory
		San Diego, CA 92152
		ATTN: Electron Materials
		        Science Division
			1

Commanding Officer Office of Naval Research Building 114, Section D 666 Summer Street Boston, MA 02210	1	Naval Missile Center Materials Consultant Code 3312-1 Point Mugu, CA 92041	1
Commanding Officer Office of Naval Research Branch Office 536 South Clark Street Chicago, IL 60605	1	Commanding Officer Naval Surface Weapons Center White Oak Laboratory Silver Spring, MD 20910 ATTN: Library	1
Office of Naval Research San Francisco Area Office 760 Market Street, Room 447 San Francisco, CA 94102	1	David W. Taylor Naval Ship Research and Development Center Materials Department Annapolis, MD 21402	1
Naval Research Laboratory Washington, DC 20375		Naval Undersea Center San Diego, CA 92132 ATTN: Library	1

ATTN: Codes 6000
              6100
              6300
              6400
              2627
	1
	1
	1
	1
	1
		Naval Underwater System Center
		Newport, RI 02840
		ATTN: Library
			1

93

BASIC DISTRIBUTION LIST (Continued)

Organization	Copies	Organization	Copies
Naval Air Development Center Code 302 Warminster, PA 18964 ATTN: Mr. F.S. Williams	1	Naval Weapons Center China Lake, CA 93555 ATTN: Library	1
Naval Air Systems Command Washington, DC 20360 ATTN: Codes 52031 52032	1	Naval Postgraduate School Monterey, CA 93940 ATTN: Mechanical Engineering Department	1
Naval Sea System Command Washington, DC 20362 ATTN: Code 035	1	NASA Headquarters Washington, DC 20546 ATTN: Code RRM	1
Naval Facilities Engineering Command Alexandria, VA 22331 ATTN: Code 03	1	NASA (216) 433-400 Lewis Research Center 21000 Brookpark Road Cleveland, OH 44135 ATTN: Library	1
Scientific Advisor Commandant of the Marine Corps Washington, DC 20380 ATTN: Code AX	1	National Bureau of Standards Washington, DC 20234 ATTN: Metallurgy Division Inorganic Materials Division	1 1
Naval Ship Engineering Center Department of the Navy Washington, DC 20360 ATTN: Code 6101	1	Director Applied Physics Laboratory University of Washington 1013 Northeast Fortieth Street Seattle, WA 98105	1
Army Research Office P.O. Box 12211 Triangle Park, NC 27709 ATTN: Metallurgy and Ceramics Program	1	Defense Metals and Ceramics Information Center Battelle Memorial Institute 505 King Avenue Columbus, OH 43201	1
Metals and Ceramics Division Oak Ridge National Laboratory P.O. Box X Oak Ridge, TN 37380	1		

Organization	Copies	Organization	Copies
Army Materials and Mechanics Research Center Watertown, MA 02172 ATTN: Research Programs Office	1	Los Alamos Scientific Laboratory P.O. Box 1663 Los Alamos, NM 87544 ATTN: Report Librarian	1
Air Force Office of Scientific Research Building 410 Bolling Air Force Base Washington, DC 20332 ATTN: Chemical Science Directorate Electronics and Solid State Sciences Directorate	1 1	Argonne National Laboratory Metallurgy Division P.O. Box 229 Lemont, IL 60439 Brookhaven National Laboratory Technical Information Division Upton, Long Island New York 11973 ATTN: Research Library	1 1
Air Force Materials Laboratory Wright-Patterson AFB Dayton, OH 45433 Library Building 50, Room 134 Lawrence Radiation Laboratory Berkeley, CA	1 1	Office of Naval Research Branch Office 1030 East Green Street Pasadena, CA 91106	1

SUPPLEMENTARY DISTRIBUTION LIST

Organization	Copies	Organization	Copies

Jack Bouchard
Northrop/PPD
100 Morse Street
Norwood, MA 02062

P. Jacobson   1
Sperry Flight Systems
P.O. Box 21111
Pheonix, AZ   1

Howard Schulien
Department 6209
Bendix Corporation
Guidance Systems Division
Teterboro, NJ 07608   1

George R. Costello
Senior Staff Engineer
Control and Electromechanical
Subdivision
Guidance and Control Division
The Aerospace Corporation
P.O. Box 92957
El Segundo, CA 90009   1

Don Bates
Honeywell, Inc.
Aerospace Division
11350 U.S. Highway 19
St. Petersburg, FL 33733   1

John Hanks
Dynamics Research Corp.
60 Concord Street
Wilmington, MA 01887   1

R. Baldwin
Honeywell, Inc.
Avionics Division
2600 Ridgway Parkway
Minneapolis, MN 55413   1

D. Riley
Systems Group, Minuteman
TRW Inc.
P.O. Box 1310
San Bernardino, CA 92402   1

Bus Brady
62-11B/1
Lockheed Missile and Space
Co., Inc.
P.O. Box 504
Sunnyvale, CA 94088   1

Professor Robert Ogilvie
Department of Materials Science
and Engineering
Massachusetts Institute of Technology
Cambridge, MA 02139

Dan Fromm
MS 1A1
Delco Electronics
7929 South Howell Avenue
Milwaukee, WI 53201   1

Dr. Glen R. Buell (D. Starks)
AFML/MBT
Wright-Patterson Air Force Base
Dayton, OH 45433   1

F. Mikoliet
Autonetics Division
Rockwell International
3370 Miraloma Avenue
Anaheim, CA 92803   1

Major George Raroha
AFAL/CC
Wright-Patterson Air Force Base
Dayton, Ohio 45433   1

SUPPLEMENTARY DISTRIBUTION LIST (Continued)

Organization	Copies	Organization	Copies
Joe Jordan Litton Guidance and Control Systems 5500 Canoga Avenue Woodland Hills, CA 91364	1	Lt. Col. Gaylord Green Capt. Ken Wernle BMO/MNNG Norton Air Force Base San Bernardino, CA 92409	1
Bob Delaney Singer-Kearfott Division 150 Totowa Road Wayne, NJ 07470	1	Dave Gold (SP-230) Rick Wilson (SP-23411) Andy Weber (SP-23411) Strategic Systems Project Office Department of the Navy Washington, DC 20390	1
Elmer Whitcomb Sperry Gyroscope Division Great Neck, NY 11020	1	Lt. Col. Larry Fehrenbacker HQ/AFSC Andrews AFB, MD	1
C. Hoenig J. Holt R. Landingham Lawrence Livermore Laboratory University of California at Berkeley Livermore, CA 94550	1	N. Stuart (MMIRME) ALC/Ogden Ogden Air Logistics Command Hill AFB Ogden, UT 84404	1
Capt. S. Craig Aerospace Guidance Metrology Center Newark Af Station Newark, OH 43055	1	Professor R. M. Latanision Massachusetts Institute of Technology 77 Massachusetts Avenue Room E19-702 Cambridge, MA 02139	1
W. Lane Hamilton Standard Windsor Locks, CN	1	Dr. Jeff Perkins Naval Postgraduate School Monterey, CA 93940	1
Dr. A. G. Evans Department Material Sciences and Engineering University of California Berkeley, CA 94720	1	Dr. R. P. Wei Lehigh University Institute for Fracture and Solid Mechanics Bethlehem, PA 18015	1
Professor H. Herman State University of New York Material Sciences Division Stony Brook, NY 11794	1	Professor H.G.F. Wilsdorf University of Virginia Department of Materials Science Charlottesville, VA 22903	1

Organization	Copies	Organization	Copies
Professor J.P. Hirth Ohio State University Metallurgical Engineering Columbus, OH 43210	1	Larry Pope Sandia National Laboratories Division 5833 Alburquerque, NM 81785	1
Professor Peter Gielisse University of Rhode Island Division of Engineering Research Kingston, RI 02881	1	Professor David Turnbull Harvard University Division of Engineering and Applied Physics Cambridge, MA 02139	1
Mr. R.W. Rice Code 6360 Naval Research Laboratory 4555 Overlook Avenue, S.W. Washington, DC 20375	1	Dr. D.P. H. Hasselman Montana Energy and MHD Research and Development Institute P.O. Box 3809 Butte, MT 59701	1
Professor G.S. Ansell Rensselaer Polytechnic Institute Department of Metallurgical Engineering Troy, NY 12181	1	Dr. L. Hench University of Florida Ceramics Division Gainesville, FL 32601	?
Professor J.B. Cohen Northwestern University Department of Material Sciences Evanston, IL 60201	1	Dr. J. Ritter University of Massachusetts Department of Mechanical Engineering Amherst, MA 01002	1
Professor M. Cohen Massachusetts Institute of Technology Department of Metallurgy Cambridge, MA 02139	1	Professor G. Sines University of California at Los Angeles Los Angeles, CA 90024	1

SUPPLEMENTARY DISTRIBUTION LIST (Continued)

Organization	Copies	Organization	Copies
Professor J.W. Morris, Jr. University of California College of Engineering Berkeley, CA 94720	1	Director Materials Sciences Defense Advanced Research Projects Agency 1400 Wilson Boulevard Arlington, VA 22209	1
Professor O.D. Sherby Stanford University Materials Sciences Division Stanford, CA 94300	1	Professor H. Conrad University of Kentucky Materials Department Lexington, KY 40506	1
Dr. E.A. Starke, Jr. Georgia Institute of Technology School of Chemical Engineering Atlanta, GA 30332	1		

DATE
ILMED
-8